



# Structural and functional comparison of magnesium transporters throughout evolution

G. A. C. Franken<sup>1</sup> · M. A. Huynen<sup>2</sup> · L. A. Martínez-Cruz<sup>3</sup> · R. J. M. Bindels<sup>1</sup> · J. H. F. de Baaij<sup>1</sup>

Received: 1 March 2022 / Revised: 22 May 2022 / Accepted: 21 June 2022 / Published online: 12 July 2022  
© The Author(s) 2022

## Abstract

Magnesium ( $Mg^{2+}$ ) is the most prevalent divalent intracellular cation. As co-factor in many enzymatic reactions,  $Mg^{2+}$  is essential for protein synthesis, energy production, and DNA stability. Disturbances in intracellular  $Mg^{2+}$  concentrations, therefore, unequivocally result in delayed cell growth and metabolic defects. To maintain physiological  $Mg^{2+}$  levels, all organisms rely on balanced  $Mg^{2+}$  influx and efflux via  $Mg^{2+}$  channels and transporters. This review compares the structure and the function of prokaryotic  $Mg^{2+}$  transporters and their eukaryotic counterparts. In prokaryotes, cellular  $Mg^{2+}$  homeostasis is orchestrated via the CorA, MgtA/B, MgtE, and CorB/C  $Mg^{2+}$  transporters. For CorA, MgtE, and CorB/C, the motifs that form the selectivity pore are conserved during evolution. These findings suggest that CNNM proteins, the vertebrate orthologues of CorB/C, also have  $Mg^{2+}$  transport capacity. Whereas CorA and CorB/C proteins share the gross quaternary structure and functional properties with their respective orthologues, the MgtE channel only shares the selectivity pore with SLC41  $Na^+/Mg^{2+}$  transporters. In eukaryotes, TRPM6 and TRPM7  $Mg^{2+}$  channels provide an additional  $Mg^{2+}$  transport mechanism, consisting of a fusion of channel with a kinase. The unique features these TRP channels allow the integration of hormonal, cellular, and transcriptional regulatory pathways that determine their  $Mg^{2+}$  transport capacity. Our review demonstrates that understanding the structure and function of prokaryotic magnesiumotropic proteins aids in our basic understanding of  $Mg^{2+}$  transport.

**Keywords** Magnesium · Channel · Transporter · CNNM · TRPM · SLC41

## Introduction

Magnesium ( $Mg^{2+}$ ) is required as co-factor in over 300 enzymatic reactions and is therefore involved in many physiological processes [1–3]. The involvement of free  $Mg^{2+}$  can be via substrate complexes or directly to the enzymes themselves and is dependent on the spatial arrangement of water molecules [2]. This is influenced by the large hydration shell, which is 400 times larger when unhydrated and larger than

other positively charged minerals, such as  $Na^+$ ,  $K^+$  and  $Ca^{2+}$  [4]. In pro- and eukaryotic cells, the majority ( $\pm 90\%$ ) of the intracellular  $Mg^{2+}$  is bound to ATP ( $MgATP$ ). Among others,  $MgATP$  is essential for ATPase function, phosphorylation events, and glycolytic enzymes [5–8]. Ionised  $Mg^{2+}$  acts as a co-factor for enzymes important for macromolecule synthesis, such as DNA/RNA polymerases and tRNA synthetases [9–11]. Moreover,  $Mg^{2+}$  plays a central role in protein synthesis. Data from *E.coli* bacteria indicate that a single ribosome contains at least 170  $Mg^{2+}$  ions [12]. In photosynthesis,  $Mg^{2+}$  is located in chlorophyll molecules and crucial for the absorption of photons that is required for ATP and  $O_2$  production, a phenomenon that supports all multicellular organisms [13]. Moreover,  $Mg^{2+}$  is an antagonist for  $Ca^{2+}$ , which is of particular importance in the regulation of ion channel activity [1].

As  $Mg^{2+}$  is central to enzymatic function and metabolism, cells require a transport system to keep  $Mg^{2+}$  levels stable. In vertebrates, the main magnesium-transporting proteins are transient receptor potential melastatin (TRPM) 6 and -7, solute carrier 41 (SLC41), cyclin M (CNNM)

✉ J. H. F. de Baaij  
jeroen.debaaij@radboudumc.nl

<sup>1</sup> Department of Physiology, Radboud Institute for Molecular Life Sciences, Radboud University Medical Center, P.O. Box 9101, 6500 HB Nijmegen, The Netherlands

<sup>2</sup> Center for Molecular and Biomolecular Informatics, Radboud Institute for Molecular Life Sciences, Radboud University Medical Center, Nijmegen, The Netherlands

<sup>3</sup> Center for Cooperative Research in Biosciences (CIC bioGUNE), Bizkaia Science and Technology Park, Derio, 48160 Bizkaia, Spain

proteins, and mitochondrial RNA splicing protein 2 (Mrs2) (Table 1). These  $Mg^{2+}$  channels and transporters often have a prokaryotic, bacterial and/or archaeal, orthologue. Although their function is to facilitate  $Mg^{2+}$  fluxes, they are also permeable for other (trace) divalent cations (Table 2). While research generally focusses on characterisation of eukaryotic  $Mg^{2+}$  transporters in mammalian cell models,

**Table 1** Overview of proteins found in prokaryotes that regulate cellular  $Mg^{2+}$  levels and their orthologue families in eukaryotes

Prokaryote	Eukaryote		
	<i>S. cerevisiae</i>	<i>Plantae</i>	<i>Metazoa</i>
Superfamilies			
CorA	Mrs2, Alr1/2, Mnr2, Lpe10	Mrs2-like proteins	Mrs2
MgtA	–	–	–
MgtE	–	MgtE-like proteins <sup>a</sup>	SLC41
CorB/C	MAM3	DUF21(-CBS) proteins	CNNMs
–	– <sup>b</sup>	–	TRPM6/7

<sup>a</sup>The MgtE orthologues have currently only been described in unicellular green and red algae (*Viridiplantae* and *Archaeplastida*, respectively) [14, 15]

<sup>b</sup>TRP channels have been described in yeast, but to date no particular orthologues of TRPM6/7 have been identified

many valuable insights can be obtained by examining their prokaryotic counterparts in greater detail. In prokaryotes, four major  $Mg^{2+}$  channels and transporters have been identified, named after their role in Cobalt resistance (Cor) and  $Mg^{2+}$  transport (Mgt): CorA, CorB/C, MgtA/B, and MgtE (Fig. 1). In recent years, structures of several prokaryotic  $Mg^{2+}$  transporters and channels have been elucidated using cryo-electron microscopy and X-ray crystallography. Not only have these structures given insights into how these transporters/channels are regulated, but also reveal the function of their eukaryotic counterparts.

In this review, we compare the structure of the prokaryotic  $Mg^{2+}$  transporting proteins and interpret the functional similarities of their eukaryotic orthologues. All  $Mg^{2+}$  transporting superfamilies will be discussed in terms of structure and functional characteristics.

## Main body

### The CorA family and the mitochondrial $Mg^{2+}$ channel Mrs2 orthologue

In 1969, two groups identified active  $Mg^{2+}$  transport in *E. coli*, which was temperature dependent, but independent of

**Table 2** Overview of prokaryotic and eukaryotic  $Mg^{2+}$  channels and transporters and their ion selectivity

Protein	Transporting mechanism	Ion selectivity	Technique [reference]
CorA	Channel	$Ca^{2+} > Mn^{2+} > Co^{2+} > Mg^{2+} > Ni^{2+}$ (in the constitutively open CorA D253K mutant)	Voltage clamp recording in oocytes [16]
Mrs2	Channel	$Mg^{2+} > Mn^{2+} > Co^{2+} > Ni^{2+} > Ca^{2+}$	Competition assay in <i>S. typhimurium</i> [17]
CorB/C	Exchanger	Not reported	Patch clamp recording in yeast [18]
CNNM2	Transporter (?)	$Mg^{2+} > Sr^{2+} = Zn^{2+} = Cd^{2+} = Ni^{2+} > Ba^{2+} = Co^{2+} > Fe^{2+} = Cu^{2+} = Mn^{2+} = Ca^{2+}$	Voltage clamp technique in oocytes [19]
CNNM3	Exchanger (?)	$Mg^{2+} > Fe^{2+} > Cu^{2+} > Co^{2+} > Ni^{2+} > Ca^{2+}$	Voltage clamp technique in oocytes [19]
MgtE	Channel	$Mg^{2+} > Mn^{2+} > Ca^{2+} > Na^{+} = K^{+}$	Liposome-based transport assays [20]
SLC41A1	$Na^{+}$ -exchanger (?)	$Mg^{2+} > Sr^{2+} = Fe^{2+} \geq Ba^{2+} = Cu^{2+} > Zn^{2+} = Co^{2+} > Cd^{2+} = Mn^{2+} = Ni^{2+} = Ca^{2+}$	Voltage clamp technique in oocytes [19]
SLC41A2	$Na^{+}$ -exchanger (?)	$Mg^{2+} > Ba^{2+} > Ni^{2+} = Co^{2+} > Fe^{2+} = Mn^{2+} = Sr^{2+} > Cu^{2+} = Zn^{2+} = Ca^{2+}$	Voltage clamp technique in oocytes [19]
SLC41A3	$Na^{+}$ -exchanger (?)	$Ba^{2+} > Mg^{2+} > Ni^{2+} = Zn^{2+} > Sr^{2+} = Fe^{2+} > Mn^{2+} > Cu^{2+} = Co^{2+} > Ca^{2+}$	Voltage clamp technique in oocytes [19]
TRPM6	Channel	$Zn^{2+} > Ba^{2+} > Mg^{2+} = Ca^{2+} = Mn^{2+} > Sr^{2+} > Cd^{2+} = Ni^{2+}$	Patch clamp recording in CHOK1 cells [21]
TRPM7	Channel	$Ba^{2+} > Ni^{2+} > Mg^{2+} > Zn^{2+} \geq Ca^{2+}$	Patch clamp recording in HEK293 cells [22]
		$Zn^{2+} = Ni^{2+} > Ba^{2+} > Co^{2+} > Mg^{2+} \geq Mn^{2+} \geq Sr^{2+} \geq Cd^{2+} \geq Ca^{2+}$	Patch clamp recording in HEK293 cells [23]
		$Ni^{2+} > Zn^{2+} > Ba^{2+} = Mg^{2+} > Ca^{2+} = Mn^{2+} = Sr^{2+} > Cd^{2+}$	Patch clamp recording in CHOK1 cells [21]
MgtA	P-type $Mg^{2+}$ -ATPase	$Zn^{2+} > Mg^{2+} > Ni^{2+} = Co^{2+} > Ca^{2+}$	Competition assay in <i>S. typhimurium</i> [17]
MgtB	P-type $Mg^{2+}$ -ATPase	$Mg^{2+} = Co^{2+} = Ni^{2+} > Mn^{2+} > Ca^{2+}$	Competition assay in <i>S. typhimurium</i> [17]

To note, two-electrode voltage clamp can only be used in relatively large in vitro models, e.g. oocytes. In addition, the intracellular compartment cannot be controlled and may therefore be not suitable to determine permeation profiles [24, 25]

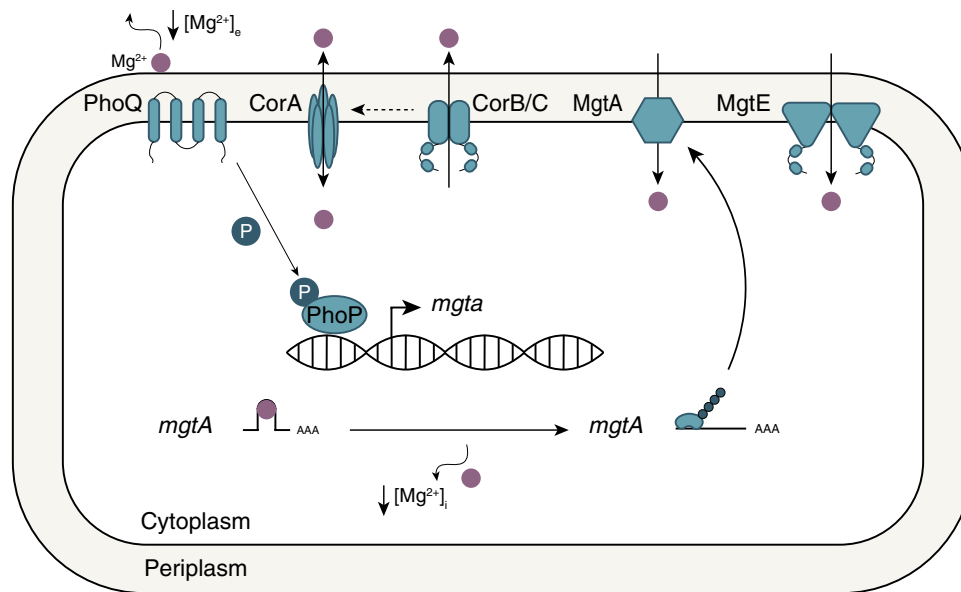


**Fig. 1** Schematic overview of prokaryotic  $Mg^{2+}$  transport proteins. Cobalt resistance (Cor) and  $Mg^{2+}$  transporting (Mgt) proteins CorA or MgtE form the major  $Mg^{2+}$  influx systems in prokaryotes. However, the channels are rarely present together in the same species, i.e. prokaryotes either have CorA or MgtE channels. CorA and CorB/C can regulate  $Mg^{2+}$  efflux from cells, although the dependency of CorA in relationship to CorB/C proteins remains unstudied. The MgtA ATPase is activated when extra- or intracellular  $Mg^{2+}$  levels are low. In response to these cues, the PhoQ/P system is activated.

Upon  $Mg^{2+}$  restriction, PhoQ phosphorylates PhoP, which in turn results in transcription of *mgta* encoding MgtA. Low intracellular  $Mg^{2+}$  concentration also enables efficient translation of the *mgta* transcript via a riboswitch. Translation results in expression of the MgtA ATPase, which hereafter localises to the membrane to regulate  $Mg^{2+}$  influx via primary active transport. The intracellular  $Mg^{2+}$  concentration is ultimately determined based on the expression of the channels/transporters at the membrane and their activity

other cations, such as calcium ( $Ca^{2+}$ ), potassium ( $K^+$ ), or manganese ( $Mn^{2+}$ ) [26, 27]. The molecular mechanism for  $Mg^{2+}$  transport was identified in the context of cobalt ( $Co^{2+}$ ) resistance. Exposure of *E. coli* to relatively high  $Co^{2+}$  levels disrupted growth, yet was inhibited in the presence of high  $Mg^{2+}$  levels [28]. Mutants that displayed resistance to  $Co^{2+}$ -mediated growth retardation also showed decreased  $Mg^{2+}$  transport, suggestive for shared uptake of these metals into bacteria [28]. The gene was identified in *Salmonella typhimurium* and named *corA* (protein: CorA) [29]. Approximately half of the prokaryotes have the orthologue and is considered one of the main channels for  $Mg^{2+}$  into cells (Fig. 1) [30]. Transport studies using radioactive  $^{28}Mg^{2+}$  also showed that CorA also allows efflux, which is dependent on the extracellular  $Mg^{2+}$  concentration [31]. Efflux was abolished upon mutagenesis of the genetic loci encoding Cobalt resistance B, C, and D (CorB, -C, and -D; literature on the characterisation of CorD is absent and will not be described further) [31, 32]. Similarly to MgtE, CorA uses the electrochemical gradient across the cytoplasmic membrane to transport its substrates [33, 34]. This dependence on the membrane potential means that the ion transport it promotes is influenced by changes in pH or by fluctuations in the concentration of other ions. CorA is, together with MgtE, the

only primary  $Mg^{2+}$  channel whose crystal structure is known in its entirety in the presence and in the absence of divalent cations ( $Mg^{2+}$  and  $Ca^{2+}$ ) [35–38].

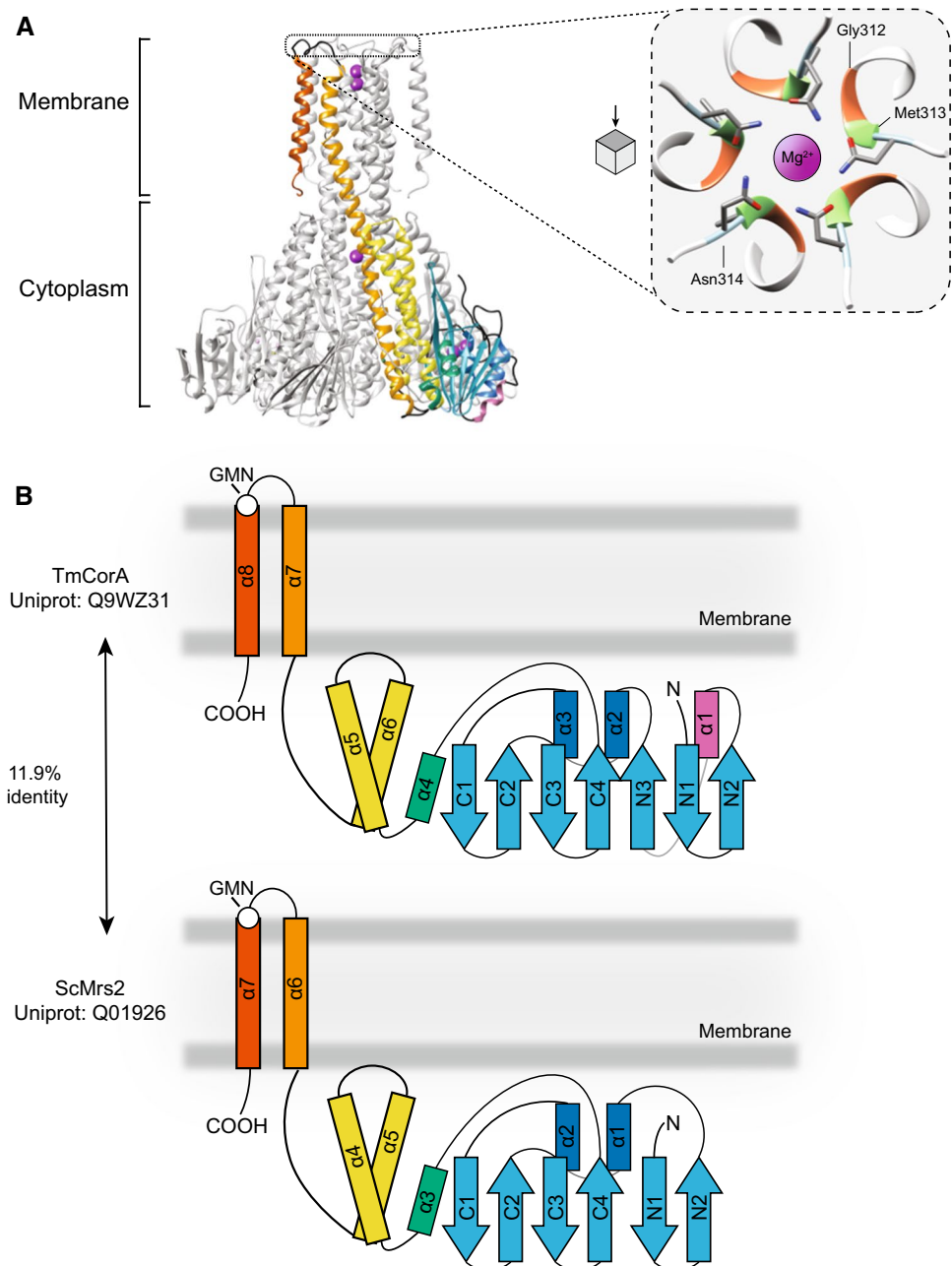
The structure of CorA was solved in the bacterium *Thermotoga maritima* (TmCorA) using X-ray crystallography [34, 39]. The protein consists of a large N-terminal region, connected to a smaller C-terminal region through a long  $\alpha$ -helix. The C-terminal region contains two transmembrane helices. To be functionally active, CorA associates with itself to form funnel-shaped homopentamers, which in total contain ten transmembrane segments. The functional unit forms a central pore that crosses the membrane and reaches the intracellular region [35, 40]. The crystal structure revealed that cations bind to both the central pore and the intracellular region. The latter has regions rich in acidic residues that are located between the different subunits, where  $Mg^{2+}$  ions bind and regulate channel activity [34, 35, 40]. In each subunit there are five  $Mg^{2+}$ -binding sites. Upon binding,  $Mg^{2+}$  ions increase the number of contacts between subunits and stabilise the closed conformation of the channel [38]. In the presence of  $Mg^{2+}$ , the pore is too narrow to allow ion entry [41]. In contrast, loss of binding of  $Mg^{2+}$ , the cytoplasmic N-terminus and gains flexibility, resulting in an asymmetric domain rearrangement. Ultimately, this allows the opening

of the pore and influx of  $Mg^{2+}$  through the channel [42]. Yet, mutagenesis of the  $Mg^{2+}$ -binding sites in TmCorA did not result in a constitutive opening of the channel, leaving the mechanistic role of  $Mg^{2+}$  in CorA gating unresolved [43]. Although the exact mechanism of opening or closing remains unknown, it has been postulated that the selectivity of CorA for  $Mg^{2+}$  is due to a conserved motif located at the entrance of the pore. This motif, defined by a YGMNFxxMPEL sequence, located at the loop of the C-terminal transmembrane alpha helices (Fig. 2) [44]. Distant orthologues of CorA lost the MPEL motif and only share the conservation

of the Gly-X-Asn (GxN) motif, of which the X represents hydrophobic amino acids Met, Val, or Ile (Fig. 2) [44]. CorA is likely permeable for hexa-hydrated  $Mg^{2+}$ , as it supports transport of  $Co^{2+}$  and  $Ni^{2+}$ , which have the approximate same size as hydrated  $Mg^{2+}$  [17, 32]. In addition, CorA could be inhibited to cobalt hexamine, a structural analogue of  $Mg^{2+}$  as it competes with  $Mg^{2+}$ -binding residues in the cytosolic pore domain [41].

During evolution, this pentameric transporter remained important for  $Mg^{2+}$  transport across all phyla (Table 1), as there are orthologues present in every phylum, as

**Fig. 2** Structure of CorA and its orthologue Mrs2; **A** Structure of the pentamer Cobalt resistance A of *Thermotoga maritima* (TmCorA, PDB: 3JCF) in complex with  $Mg^{2+}$  (purple spheres, left panel) with one monomer highlighted. Right panel: zoom in on the surface of the transmembrane domain of CorA depicting the typical GxN motif that orthologues of CorA contain.  $Mg^{2+}$  ions have been enlarged for illustration purposes. **B** Schematic depiction of the monomer of CorA (up panel) and Mrs2 (bottom panel), with the location of the GMN motif located at the surface of the pore (white dot). Same colours as in A have been used to reflect the approximate structure and location. The schematic structure of the yeast homologue Mrs2 (PDB: 3RKG) has been depicted, which is based on the cytoplasmic region



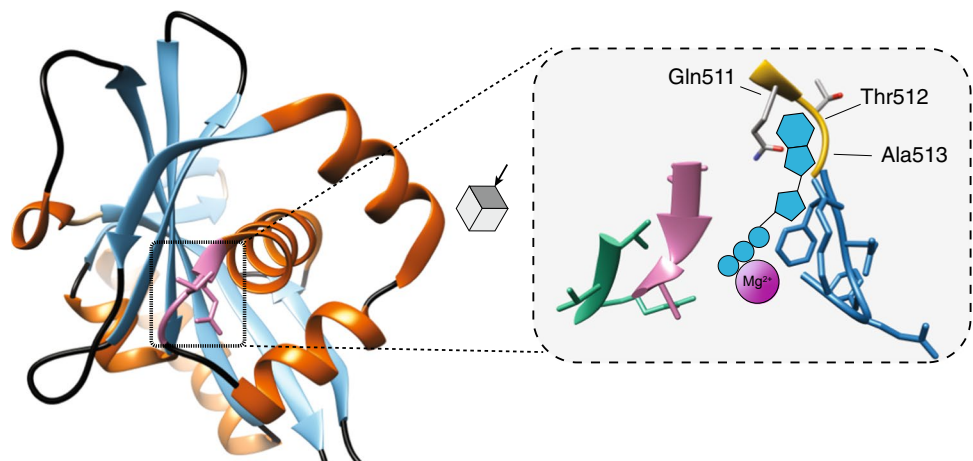
extensively described in this review [44]. The first eukaryotic orthologues of CorA were identified in *Saccharomyces cerevisiae*; mitochondrial RNA splicing protein 2 (Mrs2) and its homologue Lpe10. Both Mrs2 and Lpe10 are located in the mitochondria, possibly as a result of the endosymbiosis that gave rise to these organelles, and inactivating mutations in the genes cause decrease in  $Mg^{2+}$  content in mitochondria and cells [45–48]. The Mrs2 protein mainly shows structural conservation to CorA and has low amino acid identity to it (11.9%), apart from the typical GxN motif in the pore (Fig. 2B). The  $\alpha$ - $\beta$ - $\alpha$  sandwich at the N-terminus is similar for CorA and Mrs2, although the latter contains an extra  $\alpha$ - $\beta$  at the start of the protein [49]. Only a few residues are conserved between TmCorA and Mrs2 that are important for  $Mg^{2+}$  sensing [49]. Nevertheless, CorA expression partially alleviates the phenotype in *mrs2*-deficient yeast, highlighting the bacterial ancestry to this prokaryotic protein [46, 50]. Metazoa only contain one Mrs2 homologue, which exclusively is localised to the mitochondria [47]. Indeed,  $Mg^{2+}$  plays a role in mitochondrial processes like the citric acid cycle, reactive oxygen species (ROS) production, and apoptosis [51, 52]. In contrast to metazoa, many Mrs2 orthologues are present in plants, such as in *Arabidopsis thaliana*, containing ten genes encoding orthologues of Mrs2 (*ARATH;Mgt*), which may be due to independent gene duplications (TF328433) [53]. *Arabidopsis Mrs2* is able to complement, at least to an extent, the growth of *mrs2* mutant *S. cerevisiae* grown in  $Mg^{2+}$  deficient conditions [54]. It is still not understood why many plants have multiple orthologues of Mrs2, although this may be explained by the spatial specific expression pattern [55–57]. Moreover, deficiency of one of the genes often leads to growth retardation, indicating that these proteins are non-redundant [54, 58].

### The $Mg^{2+}$ transporting ATPase MgtA/B and orthologues

Studies demonstrating  $Mg^{2+}$  influx in bacteria demonstrated that the kinetics of  $Mg^{2+}$  transport changed based on the exposure to different extracellular  $Mg^{2+}$  concentrations [29]. Concentrations as low as 10  $\mu\text{mol/L}$  were sufficient for bacterial growth and increased the  $V_{\text{max}}$  of  $Mg^{2+}$  transport, suggesting there was more than one influx mechanism at hand. This observation ultimately led to the discovery of the *mgtA* and *mgtCB* loci in *S. typhimurium*, encoding for MgtA and MgtB/C, respectively [32].

The MgtA/B proteins belong to the P-type ATPase superfamily, which also includes the  $\text{Na}^+/\text{K}^+$ -ATPase and the  $\text{Ca}^{2+}$ -ATPase, and use ATP hydrolysis to fuel  $Mg^{2+}$  transport [7]. *S. typhimurium* strains containing either wild-type MgtA or MgtB and mutant CorA displayed significant  $Mg^{2+}$  influx when exposed to 20  $\mu\text{mol/L}$   $Mg^{2+}$ , with both MgtA and -B having a similar  $K_m$  as CorA in *S. typhimurium* [17]. Expression of the *mgtA* and *mgtCB* loci is modulated by the PhoQ/P two-component system, a phosphorylation relay that regulates virulence, pH, osmolality-induced stress, and  $Mg^{2+}$  deficiency (Fig. 1) [59–61]. The membrane receptor PhoQ phosphorylates the transcription factor PhoP when extracellular  $Mg^{2+}$  concentrations decrease. This initiates transcription of, among others, the *mgtA* and *mgtCB* loci. In addition, the 5' untranslated region (5'UTR) of *mgtA* undergoes conformational changes when intracellular  $Mg^{2+}$  levels are low as consequence of the release of  $Mg^{2+}$  ions of mRNA molecule and initiation of translation, a phenomenon known as riboswitch [62, 63]. This has led to the general belief that  $Mg^{2+}$  influx is mainly regulated by CorA, but is promoted by MgtA/B upon  $Mg^{2+}$  deprivation.

**Fig. 3** Structure of the N-terminus of MgtA. Structure of the N-terminus of Magnesium Transporter A (MgtA) of *Escherichia coli* (MgtA, PDB: 3GWI). Right panel: zoom in on the surface of the MgATP-binding site with the four binding motifs. The xTG (yellow) is unique to the MgtA protein compared to members of the P-type ATPases. MgATP has been enlarged for illustration purposes and does not reflect the physical bindings sites with the protein





Elucidation of the structure of the N-terminus of MgtA revealed the X-Thr-Gly motif (xTG), with X coding for Asn, Asp, Gln, or Glu, which is likely involved in binding of the MgATP (Fig. 3) [64]. This motif is one of the four ATP-binding motifs in MgtA and is unique compared to Ca<sup>2+</sup> and Na<sup>+</sup>/K<sup>+</sup>-ATPases and shared in many of the MgtA homologues in various prokaryotes. In MgtB, the Thr is replaced by Ser in *S. typhimurium* (QSG) [64]. It has been postulated that QSG could result in higher affinity for the MgATP nucleotide base compared to the xTG motif, but this has not been experimentally validated yet. Further characterisation of the MgtA/B protein structure is needed to understand the role of its unique motif in Mg<sup>2+</sup> transport.

Although Mg<sup>2+</sup>-ATPases have been postulated in vertebrates, the molecular identity of a MgtA/B orthologue remains obscure. Many studies reported Mg<sup>2+</sup>-dependent ATP hydrolytic activity in different organelles, such as the plasma membrane, endoplasmic reticulum, sarcolemma, and microvesicles found in heart, muscle, and brain [65–70]. This may suggest the presence of a Mg<sup>2+</sup>-ATPase, yet studies focussing on Mg<sup>2+</sup> transport by these Mg<sup>2+</sup>-dependent ATPases are limited. Searching for orthologues of MgtA, homology detection using HHpred suggested that members of the ATPase 13 in human could be an interesting candidate [71, 72]. Inactivation of the *ATP13A4* gene was associated with delayed language development and in overexpression in cells stimulates Ca<sup>2+</sup> influx [73, 74]. Members of the ATP13 family transport a range of electrolytes or organic compounds, such as Ca<sup>2+</sup>, Mn<sup>2+</sup>, or polyamines [75–77]. Interestingly, Claudin 16 knock-out mice, a model that induces renal-mediated Mg<sup>2+</sup> wasting, showed increased gene expression of *Atp13a4* in the kidney [78]. In *C. elegans*, the orthologue of human ATP13A2, CATP-6, was found to regulate GON-2 [79]. GON-2 is the orthologue of the Mg<sup>2+</sup> channel TRPM6 and -7 in vertebrates, proteins that will be discussed in detail later. Functional assays, preferably with purified ATP13A4 protein, could reveal whether these proteins could transport Mg<sup>2+</sup> and are the orthologues of MgtA/B.

### The cellular Mg<sup>2+</sup> channel MgtE and its vertebral orthologue SLC41

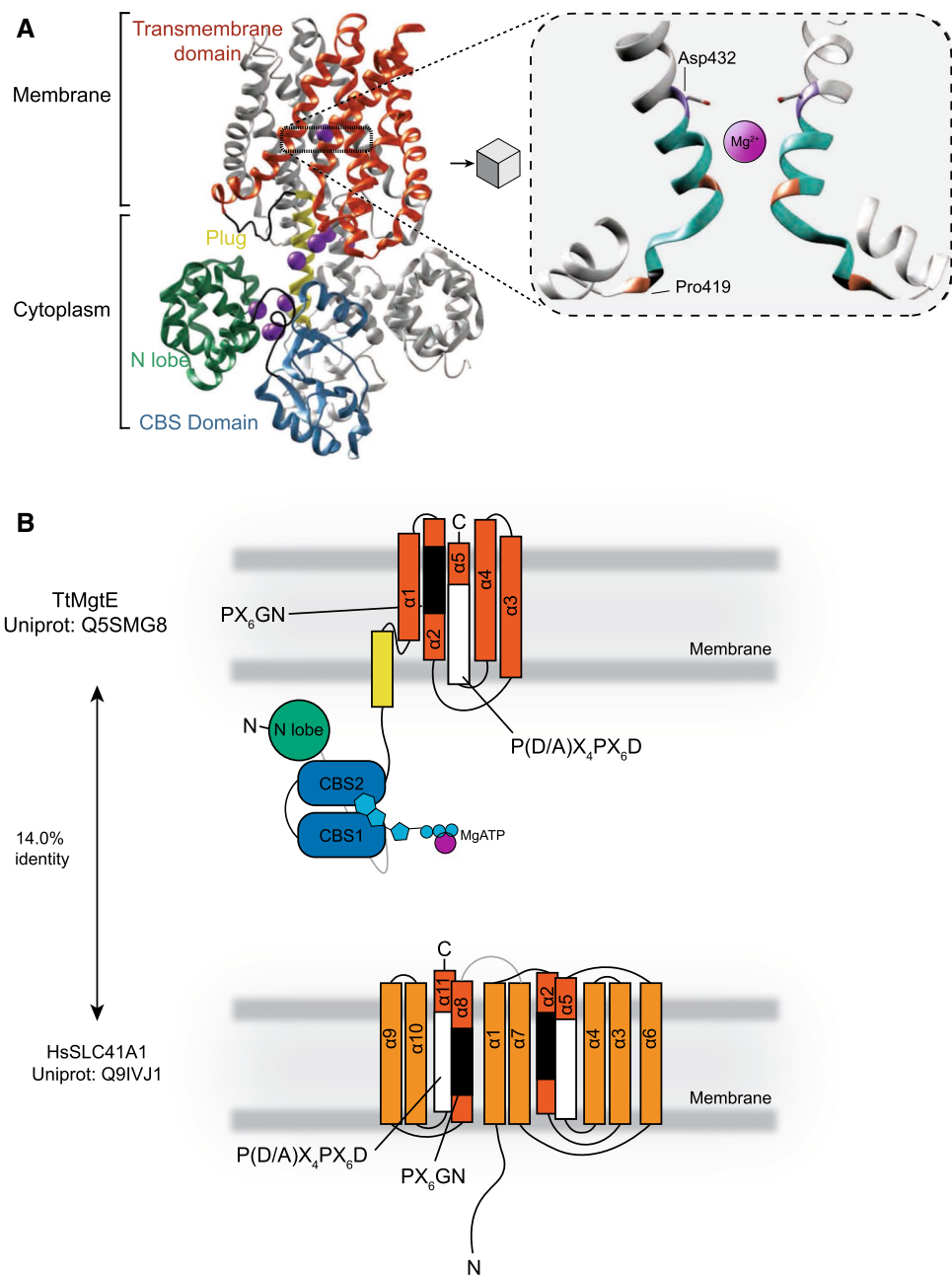
In a *corA*, *mgtA*, and *mgtCB* deficient *S. typhimurium* MM281 strain, a genomic library was expressed of the Gram-positive *Bacillus firmus* to identify additional Mg<sup>2+</sup> transporters [80]. Cells that showed growth under Mg<sup>2+</sup> deprived conditions were selected for further genetic analysis, which led to the discovery of the *mgte* locus [80]. The MgtE Mg<sup>2+</sup> channel is present in both *Bacteria* and *Archaea*, although it appears to be largely absent in prokaryotes that express CorA (Fig. 1) [81]. Interestingly, the Gram-negative bacteria *Dechloromonas aromatica* and *Magnetospirillum magnetotacticum* contain CorA homologues that are unusually long

and have a N-terminus that exhibits homology to MgtE [44]. Just as CorA, MgtE is a non-selective cation channel, facilitating influx of Mg<sup>2+</sup>, Zn<sup>2+</sup>, Co<sup>2+</sup>, and Ni<sup>2+</sup> [80]. Similar to *mgtA*, the *mgte* transcript undergoes structural changes via a riboswitch upon Mg<sup>2+</sup> deprivation, controlled by a tertiary structure called the M-box [82]. However, the M-box is not present in every species that expresses MgtE. For instance, *Bacillus halodurans*, *B. subtilis*, *Clostridium acetobutylicum*, *Vibrio cholerae*, and *Chromobacterium violaceum* have the M-box upstream of *mgte*, whereas this is absent in the *mgte* transcripts in *S. aureus*, *Cornebacterium glutamicum*, *Mycobacterium bovis* and *T. maritima*.

MgtE adopts a homodimeric structure that differs structurally from the CorA proteins (Fig. 4A) [83]. The C-terminal tail contains cystathionine β-synthase (CBS) domains that are found in various proteins including chloride channels and AMP-activated protein kinase (AMPK). The CBS domains are heavily conserved and found in all phyla, with over 50 proteins in *H. sapiens* [84]. The domain in MgtE binds MgATP and has a dissociation constant (K<sub>d</sub>) for ATP of approximate 172 μmol/L, suggesting that MgATP is usually bound to the CBS domains as cytosolic ATP levels in vivo are in the millimolar range [85]. Additionally, Mg<sup>2+</sup> ions bind to the N-lobe and plug (Fig. 4A), which is involved in the gating mechanism of the protein. Decreased intracellular Mg<sup>2+</sup> levels give flexibility to the N-lobe and the plug, ultimately resulting in opening of the pore [20, 83, 86, 87]. The transmembrane spanning domains contain conserved D1 and D2 domains, defined by PX<sub>6</sub>GN and P(D/A)X<sub>4</sub>PX<sub>6</sub>D motifs, respectively. Located at helices TM2 and -5, these domains contribute to the specificity for cation transport of the MgtE proteins [81, 88, 89]. In MgtE, the N-lobe and plug contain Mg<sup>2+</sup>-bindings sites and are important for gating [20, 83, 86]. Through a strong interaction of the plug with the transmembrane, particularly TM2 and -5, the pore is closed. Loss of Mg<sup>2+</sup> disrupts the association of the plug with TM2 and -5, ultimately leading to opening of the pore. The interaction of the N-lobe and CBS domains is ambiguous and disordered in Mg<sup>2+</sup>-free.

In 2003, bioinformatical approaches led to the identification of the solute carrier family 41 (SLC41) in humans, mouse, and *C. elegans*, which is the eukaryotic homologue of MgtE [89]. Interestingly, MgtE orthologues have not been found in land plants, fungi and brown or red seaweed (Fig. 5) [15]. The identified proteins are homologous to the transmembrane spanning helices found in MgtE with the conserved motifs PX<sub>6</sub>GN and P(D/A)X<sub>4</sub>PX<sub>6</sub>D (Fig. 4B) [89]. The family has three members: SLC41A1, SLC41A2, and SLC41A3. The SLC41 family contains two times the PX<sub>6</sub>GN and P(D/A)X<sub>4</sub>PX<sub>6</sub>D motifs, allow to proteins to potentially function as monomers or dimers to facilitate Mg<sup>2+</sup> transport, similarly to the prokaryotic MgtE proteins [90]. The double motifs are only present in *Archaea*, choanoflagellates,

**Fig. 4** Structure of MgtE and its orthologue SLC41A1; **A** Structure of the dimer *Thermus thermophilus* Mg<sup>2+</sup> transporter TtMgtE (PDB: 2ZY9) in complex with Mg<sup>2+</sup> (purple spheres, left panel) with one monomer highlighted. Right panel: zoom in on the pore of MgtE depicting the typical P(D/A)X<sub>4</sub>PX<sub>6</sub>D motif that orthologues of MgtE contain. Both MgtE and solute carrier family 41 A 1 (SLC41A1) have the PX<sub>6</sub>GN and P(D/A)X<sub>4</sub>PX<sub>6</sub>D motifs. Mg<sup>2+</sup> ions have been enlarged for illustration purposes. **B** Schematic depiction of the monomer of MgtE (upper panel) and SLC41A1 (bottom panel), with the approximate location of the PX<sub>6</sub>GN (black) and P(D/A)X<sub>4</sub>PX<sub>6</sub>D (white) domains. Same colours as in A have been used to reflect the approximate structure and location. The schematic structure of the human homologue SLC41A1 has been depicted, which has been based on the estimated structure using AlphaFold(AF-Q8IVJ1-F1)



and metazoa, while uni- and multicellular algae and (cyano) bacteria share contain only one PX<sub>6</sub>GN and P(D/A)X<sub>4</sub>PX<sub>6</sub>D motif. In addition, the MgtE orthologues in *Archaea* and metazoa do not contain the CBS domains and the structure of the SLC41 family deviates considerably from the MgtE proteins (Fig. 4). In addition, bacterial MgtE orthologues act as a Mg<sup>2+</sup> channel, while SLC41 family members have been reported to work as Na<sup>+</sup>/Mg<sup>2+</sup> antiporters [89–94]. Taken together, this suggests that archaeal and metazoan MgtE/SLC41 orthologues have taken a different evolutionary path. Detailed knowledge on the structure is absent, yet it is clear that the SLC41 family is distinct from MgtE proteins and

might be differently regulated. To investigate this, large-scale comparative, genomic analyses coupled to experimental studies are required to search for orthologues in different phyla, which to date are limited. This could enable the field to study in depth the evolutionary relationship between SLC41 proteins and MgtE on a genomic level, while also offering opportunities for further biochemical and functional characterisation.

Electrophysiological studies in *Xenopus laevis* oocytes demonstrated Mg<sup>2+</sup> elicited currents upon mouse SLC41A1 overexpression, yet other divalent cations, such as Zn<sup>2+</sup>, Fe<sup>2+</sup> and Cu<sup>2+</sup> were also transported [91]. Transformation with

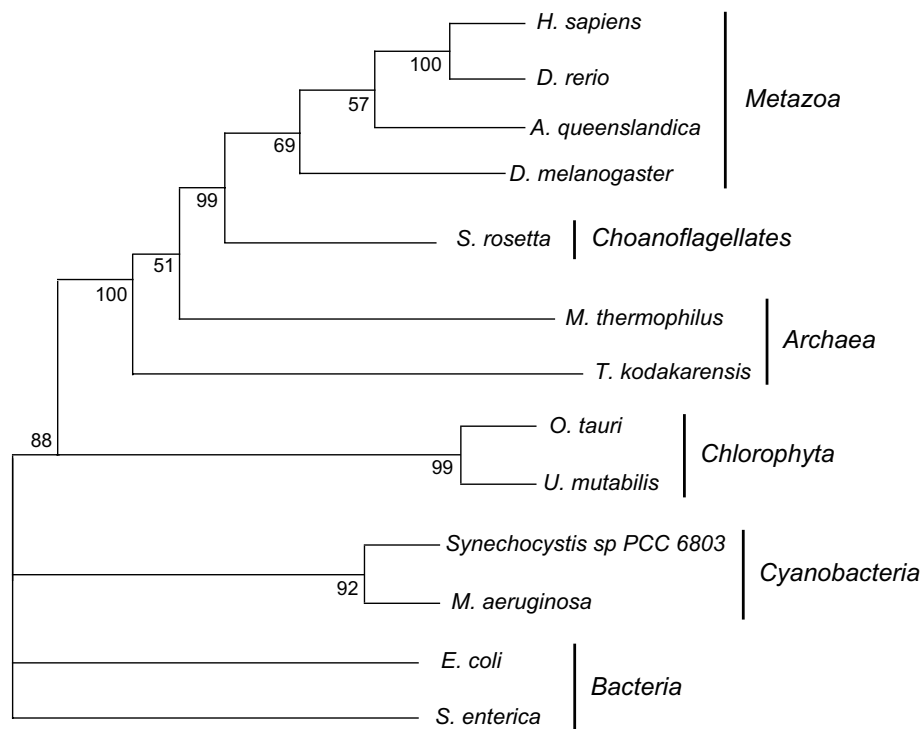


**Fig. 5** Phylogenetic tree of SLC41A1 orthologues. SLC41A1 orthologues are shared in all phyla, but limitedly in the *Plantae* kingdom. SLC41 orthologue sequences were searched with NCBI DELTA-BLAST, on Uniprot or ORCAE. Proteins sequences were then submitted to Pfam to confirm the presence of the conserved MgtE domain. Subsequently, a phylogenetic tree was constructed by maximum likelihood (bootstrap=100) using MEGA11 [95]. Used sequences for SLC41A1 orthologues: *Homo sapiens*: NP\_776253.3 (NCBI); *Danio rerio*: XP\_002663867.1 (NCBI); *Drosophila mel-*

*nogaster*: NP\_001259335.1 (NCBI); *Amphimedon queenslandica*: P\_003384010.3 (NCBI); *Salpingoeca rosetta*: XP\_004993672.1 (NCBI); *Ostreococcus tauri*: XP\_003084242.2 (NCBI); *Methanococcus thermophilus*: SDK06600.1 (NCBI); *Synechocystis sp PCC 6803*: WP\_010872029 (NCBI); *Ulva mutabilis*: UM021\_0210.1 (ORCAE); *Escherichia coli*: A0A6M0PR42 (Uniprot). *Microcystis aeruginosa*: WP\_052276493.1 (NCBI); *Thermococcus kodakarensis*: BAD85647.1 (NCBI); *Salmonella enterica*: A0A5U8SZT2 (NCBI). Branches were multifurcated when bootstrap values were <50

pUC18 human SLC41A1 plasmids in the *S. typhimurium* MM281 strain, which is deficient in *corA*, *mgtA*, and *mgtCB*, displayed superior growth in  $Mg^{2+}$  depleted conditions compared to the those with empty pUC18 plasmids [92]. Expression of SLC41A1 resulted in decreased intracellular  $Mg^{2+}$  using the fluorescent-sensitive probe Mag-Fura-2. Moreover,  $Mg^{2+}$  extrusion was abrogated upon  $Na^+$  removal, suggesting a  $Na^+/Mg^{2+}$  exchange function to facilitate  $Mg^{2+}$  extrusion [93]. Also for SLC41A2 and -A3,  $Na^+$ -dependent  $Mg^{2+}$  transport has been observed [94, 96], yet cation specificity may differ between family members [97]. In contrast, Arjona et al. observed both  $Na^+$ -independent  $Mg^{2+}$  uptake and extrusion using the stable isotope  $^{25}Mg^{2+}$  [98], leaving the molecular mode of action of the SLC41 members to be elucidated. However, studies in vivo observed a clear role for SLC41A1 and A3 in systemic  $Mg^{2+}$  homeostasis. Knock-down of *slc41a1* in zebrafish larvae decreased the  $Mg^{2+}$  content and induced a transcriptional response of genes involved in  $Mg^{2+}$  homeostasis [98]. *Slc41a3* expression was increased in kidneys of mice fed with low- $Mg^{2+}$  diets and *Slc41a3*<sup>-/-</sup> mice displayed hypomagnesaemia and increased intestinal  $Mg^{2+}$

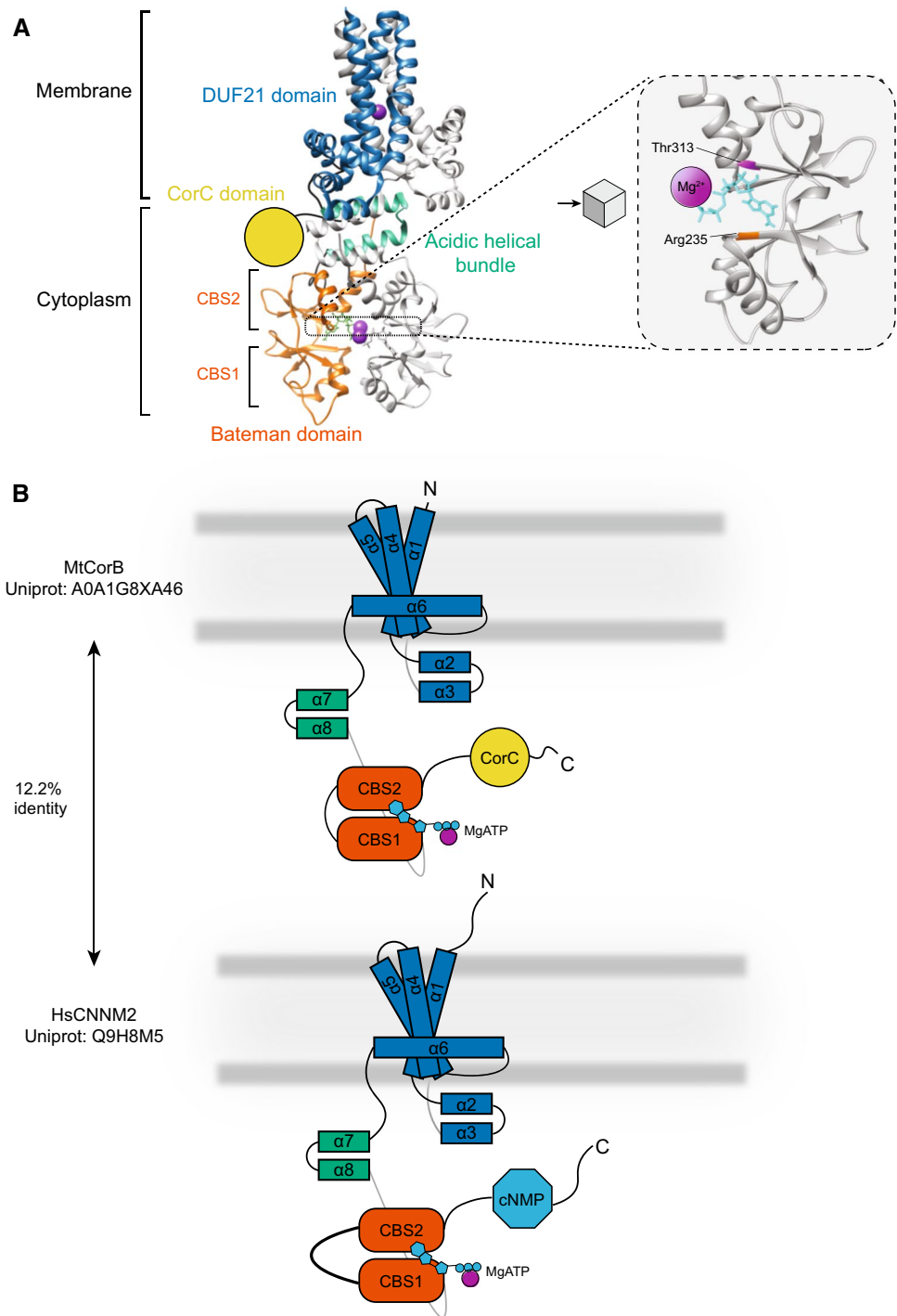
absorption [99, 100]. Yet, how SLC41A3 contributes to  $Mg^{2+}$  homeostasis remains to be elucidated. While SLC41A1 and -A2 are located at the plasma membrane, SLC41A3 is predominantly found in the mitochondria [90, 94, 98]. To date, no causal link has been made between mitochondrial  $Mg^{2+}$  transport and systemic  $Mg^{2+}$  homeostasis.

### The $Mg^{2+}$ efflux proteins CorB/C and orthologue CNNM proteins

Although CorA was initially thought to be involved in both  $Mg^{2+}$  influx and efflux, three other genes were identified in *S. typhimurium*; *corB*, *corC*, *corD* (Fig. 1). These loci were initially identified in a screen for  $Co^{2+}$  resistance [31]. While CorA was essential for  $Mg^{2+}$  efflux, individual or combined inactivation of *corB*, *corC*, and *corD* disturbed efflux in bacteria that were preloaded with  $^{28}Mg^{2+}$  [31]. These three loci have a low level of identity with CorA, yet CorB and CorC display high similarity, with both containing CBS domains (Fig. 6). Functional and structural characterisation of CorD proteins have not been described



**Fig. 6** Structure of CorB and orthologue CNNM2; **A** Structure of the pentamer *Methanococcus thermophilus* Cobalt of resistance CorB MtCorB (PDB: 7M1T) in complex with  $Mg^{2+}$ -ATP (purple spheres, left panel) with one monomer highlighted. Right panel: zoom in on residues of the CBS domain that bind  $Mg$ ATP. Residues highlighted are homologues to human Cyclin M2 (hCNNM2) associated hypomagnesaemia, seizure, intellectual disability (HSMR) syndrome Thre568Ile (MtCorB-p.Thr313) and hCNNM4 associated Jalili syndrome Arg407Leu (Mt-CorB-p. Arg235). **B** Schematic depiction of the monomer of CorB (upper panel) and CNNM2 (bottom panel) using same colours as in A to reflect the approximate structure and location. The schematic structure of the human homologue has been depicted, which has been based on the estimated structure using homology modelling of CorB, as illustrated in Chen et al. (2021) [101]



to our knowledge, so its role in  $Mg^{2+}$  transport remains unknown. The pore of the protein is located in the domain of unknown function (DUF)21, a structure that is poorly characterised in terms of distribution among species and function [101, 102]. The C-terminal end of the protein also contains a CorC domain of unknown function. Expression of the archaeal *Methanococcus thermophilus* CorB (MtCorB) and bacterium *Tepidiphilus thermophilus*

(TtCorB) in liposomes showed transport of  $Mg^{2+}$  [101]. Expression of CorC in human embryonic kidney (HEK)293 cells showed  $Mg^{2+}$  extrusion when cells were exposed to  $Na^+$ , which was prevented when  $Na^+$  was removed from the buffer. Mutational analysis of the *Thermus parvatiensis* CorC orthologue indicated that residue Asn94 (N94) might be important for  $Na^+$  sensitivity. Indeed, mutagenesis of this residue showed decreased efflux compared to wild type

when overexpressed in HEK293 cells, being indicative that CorB/C might work as a  $\text{Na}^+/\text{Mg}^{2+}$  antiporter [102].

The vertebrate orthologues of CorB were first identified in mouse, and named ancient conserved domain protein (ACDP) 1–4, which later were renamed as Cyclin M(CNNM)1–4 [103, 104]. Earlier studies suggested a nuclear function of the protein [103], more recent evidence indicates that it acts as a  $\text{Mg}^{2+}$  transporter in metazoa. Electrophysiological studies in *X. laevis* oocytes suggested that CNNM2 acts indeed as a  $\text{Mg}^{2+}$  exchanger [105]. Additionally, studies in HEK293 cells using the  $\text{Mg}^{2+}$  probe MagnesiumGreen demonstrated  $\text{Mg}^{2+}$  extrusion upon CNNM2 overexpression [106]. However, CNNM2 overexpression in HEK293 cells could only induce small  $\text{Mg}^{2+}$  and  $\text{Zn}^{2+}$ -sensitive  $\text{Na}^+$  currents, which were ablated when a patient-derived CNNM2 mutant was used [107]. In addition, other groups could not repeat the results using the  $\text{Mg}^{2+}$ -sensitive probe Mag-Fura-2 and failed to demonstrate changes in intracellular  $\text{Mg}^{2+}$  levels upon overexpression [108]. Moreover, transport studies with the stable isotope  $^{25}\text{Mg}^{2+}$  could not detect  $\text{Na}^+$ -dependent  $\text{Mg}^{2+}$  transport in HEK293 cells [109]. Consequently, a  $\text{Mg}^{2+}$  sensor role for CNNM proteins was hypothesised. However, the  $\text{IC}_{50}$  value for  $\text{MgATP}$  binding of CNNM2 and CNNM4 are estimated to be approximately 160 and 45  $\mu\text{mol/L}$ , respectively [110, 111]. It is, therefore, difficult to imagine that these proteins sense  $\text{Mg}^{2+}$  in the physiological situation.

The role of CNNM proteins remains disputed and has been discussed elaborately earlier [110, 111]. It should be mentioned that the different views may be dependent on the interpretation of findings using different in vitro models. Using magnesium sensitive probes, such as Magnesium-Green and Mag-Fura-2, allows the determination of acute responses of CNNM protein upon various interventions, yet requires non-physiological concentrations of  $\text{Mg}^{2+}$ . In contrast, studies using the stable isotope  $^{25}\text{Mg}^{2+}$  are superior in investigating  $\text{Mg}^{2+}$  fluxes, but do not provide information on intracellular  $\text{Mg}^{2+}$  concentrations. In addition, only overexpression studies have been performed that may not reflect the physiological situations. Recently, interaction partners have been identified that can modulate CNNM function. Cell-specific expression of these proteins could exert different effects based on the model used. For instance, phosphatase of regenerating liver (PRL)1–3 are proto-oncogenic proteins that can bind to CNNM proteins and are postulated to inhibit CNNM-mediated  $\text{Mg}^{2+}$  efflux [112–114]. Translation of the PRL proteins is induced upon a decrease in the intracellular  $\text{Mg}^{2+}$  levels [115], which could then inhibit CNNM-mediated efflux. The ADP-ribosylation factor-like proteins (ARL) 15 has recently been found to be involved in the glycosylation of the CNNM2 and CNNM3 and decreased CNNM3-mediated  $^{25}\text{Mg}^{2+}$  uptake upon overexpression [116]. A recent study has shown that CNNM proteins can interact with the  $\text{Mg}^{2+}$  channel transient receptor potential receptor type 7 (TRPM7)

in vivo and in vitro.[117] ARL15 reduced TRPM7-mediated currents in *X. laevis* oocytes upon heterologous overexpression, suggesting a potential, complex regulatory mechanism of ARL15-CNNM regulation on TRPM7 channel activity.

How the CNNM protein exert their function still remains to be determined, yet from a physiological point of view, it is clear for CNNM2 and CNNM4 that they are involved in systemic  $\text{Mg}^{2+}$  homeostasis. Patients suffering dominant mutations in the *CNNM2* gene present with hypomagnesaemia, seizures, and intellectual disability (HSMR) syndrome [107, 118, 119]. Patients have increased renal  $\text{Mg}^{2+}$  wasting, fitting with the expression of CNNM2 in the distal convoluted tubule within the nephron [107, 109, 118]. Systemic and kidney-specific knockout of *Cnnm2* in murine models and knock-down in zebrafish larvae have shown to result in mild hypomagnesaemia [120, 121]. Patients with recessive mutations in CNNM2 also suffer from brain abnormalities, such as demyelination and ventricular defects [118, 122]. *Cnnm2* knock out are embryonically lethal and may suffer exencephaly [121]. Similarly, *Cnnm4* knock mice also develop hypomagnesaemia, which is attributed to intestinal malabsorption [123, 124]. It is expressed at the basolateral membrane of colonic enterocytes and facilitates  $\text{Mg}^{2+}$  extrusion towards the blood compartment. Interestingly, patients suffering Jalili syndrome due to dominant mutations in the *CNNM4* gene do not develop serum  $\text{Mg}^{2+}$  disturbances, rather defects in amelogenesis and cone-rod dystrophy [125, 126].

Structurally, CNNM proteins are similar to CorB/C (Fig. 6B) [101, 102]. The CNNM orthologues contain multiple functional domains. At the N-terminus, a relatively long peptide sequence encodes for a signal peptide domain, that is cleaved off at the endoplasmatic reticulum and subsequently degraded [109, 119]. The proteins are then targeted to the plasma membrane after glycosylation which likely takes place in the Golgi-apparatus, mediated via ARL15 [116]. The transmembrane domain, the DUF21 domain, consists of three transmembrane spanning helices. A fourth domain, located between helices 1 and 2 was predicted to be a short re-entrant loop [109]. The structure for CorB/C proteins has recently been solved and has shown that this juxtamembrane domain forms a belt-like structure around the three transmembrane domains [101, 102]. The intracellular domain of CNNM proteins has extensively been studied. Similar to  $\text{MgTE}$ , CNNM proteins and CorB/C proteins contain CBS domains that bind  $\text{MgATP}$  [106, 127–129]. Binding of both,  $\text{MgATP}$  and free  $\text{Mg}^{2+}$  ions, results in conformational changes, rendering the protein in closed. The CNNM protein subsequently contains cyclic nucleotide bind homology (CNBH) domains which, in contrast with the initial predictions (so their name), do not bind cyclic nucleotides, and perhaps regulate the function of CNNMs [128, 130]. It has been proposed that this domain I) limits the conformational changes of the CBS domains upon

binding of  $Mg^{2+}/MgATP$  or II) functions as an adaptable regulator itself [128, 130]. One of the main differences with the CorB/C proteins is that the CNNMs have an extra transmembrane helix, that acts as a signal peptide and is cleaved off at the ER membrane, which is absent in CorB/C proteins (Fig. 6B) [109]. This results in a long N-terminal domain which is glycosylated and exposed to the extracellular space. In addition, studies have shown that the linker of the CBS1 and CBS2 domains is a target for binding of proteins such as PRL1-3 and ARL15 [112–114, 116]. Interaction partners of CorB/C proteins have yet to be identified, so it is not completely certain that these prokaryotic proteins are regulated in a similar fashion as the CNNM proteins. Furthermore, the CNBH domain has replaced the CorC domain in the CNNMs. Contrary to its name, it does not bind cyclic nucleotides, but is involved in dimerisation of the proteins and facilitating the conformational changes of the CBS domains, which (indirectly) affect  $Mg^{2+}$  efflux [128, 130]. The role of CorC domains in the CorB/C proteins in its function has not been studied thus far.

Apart from its homology to the CorB/C proteins, it is intriguing to mention a potential evolutionary link between MgtE and CNNMs as both proteins form dimers and contain CBS domains. It is interesting to speculate that MgtE split in two different proteins during evolution; into the  $Mg^{2+}$  transporting proteins SLC41 and the  $Mg^{2+}$  sensors CNNMs. However, as elaborately reviewed earlier [131], structural knowledge of the CBS domains gives us insights that do not support this theory. Although both proteins bind  $MgATP$  at the CBS domains, the structural consequences are quite different. First of all, the location of the ligand binding in the CBS domains is not conserved in the two proteins. While the motif where  $MgATP$  within the CBS domains binds is present in both proteins,  $MgATP$  binds at another site within the CBS domains in MgtE, unlike in CNNMs [85, 86]. This was discovered due to identification of mutations in CNNM4 (CNNM4-p.R407L) and CNNM2 (CNNM2-p.T568I) that cause the congenital disorders Jalili and HSMR syndrome, respectively [107, 118, 129]. Second, CNNM and MgtE proteins bind ATP and  $Mg^{2+}$  in a different manner [131]. Patch clamp studies in proteoliposomes indicated that the ability of intracellular  $Mg^{2+}$  to close the MgtE channel is dependent on the presence of ATP [85]. This suggests that presence of ATP determines  $Mg^{2+}$ -sensitive gating of MgtE channels. Conversely, studies using a surface plasmon resonance sensorgram with immobilised, recombinant CBS domains from CNNM2 demonstrated binding of ionised  $Mg^{2+}$  to the CBS domains [106]. In contrast, ATP only binds in the presence of  $Mg^{2+}$ . Taken together, these findings suggest that MgtE binds  $Mg^{2+}$  in an ATP-dependent manner, while conversely CNNMs bind ATP in a  $Mg^{2+}$  dependent fashion. Thirdly, only four  $Mg^{2+}$ -bindings sites have been identified in CNNM orthologue, while MgtE contains seven. Lastly, binding of

$MgATP$  leads to “opening and closing” of the MgtE pore via the plug, while the CBS domains in CNNM adopt a “disc-like-flat” structure, which moves the DUF21 domain and closes the pore [85, 86, 101, 102, 114, 127, 130, 132]. Although these facts do not support MgtE as ancestor for the CNNM proteins, it cannot be ruled out that in time, MgtE orthologues adopted similar  $MgATP$ -binding properties as the current CNNMs.

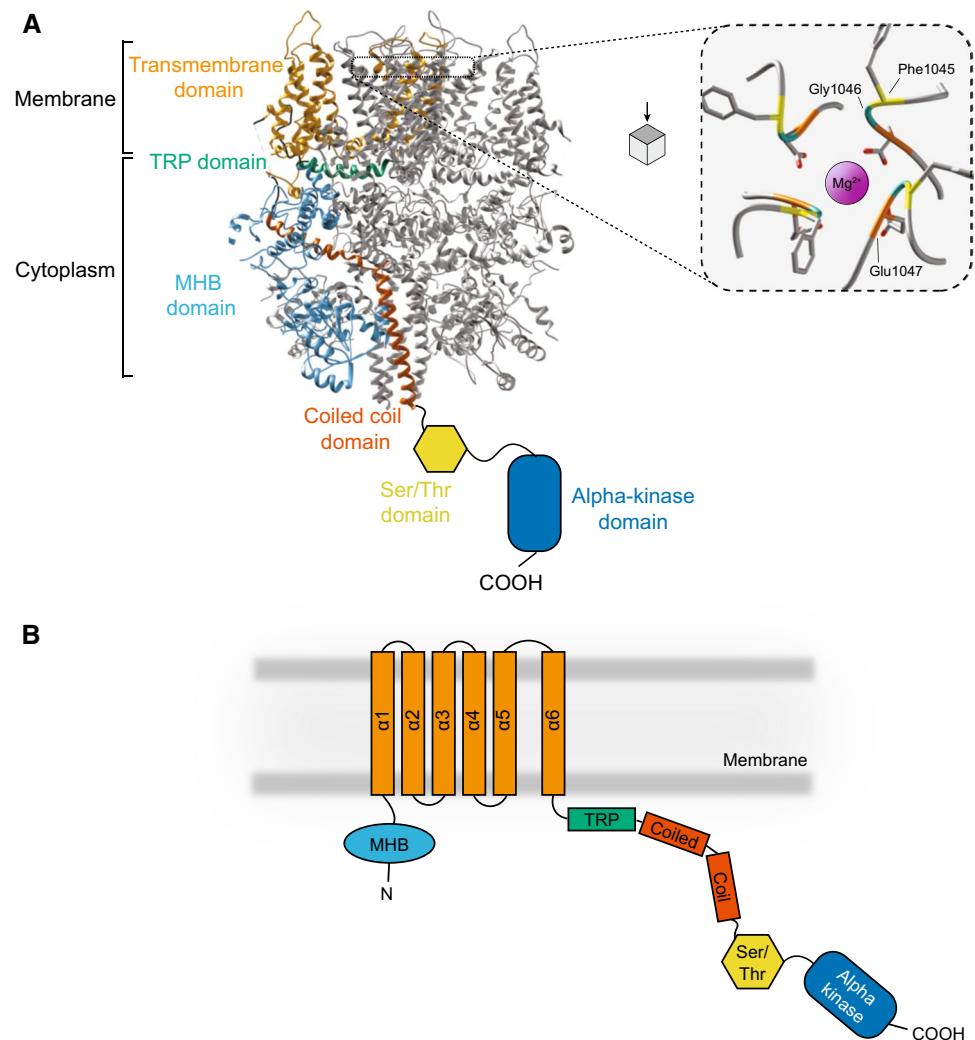
### The eukaryotic $Mg^{2+}$ channels TRPM6/7

The main entrance for  $Mg^{2+}$  into metazoan cells is via the transient receptors potential melastatin type (TRPM) 6 and 7 channels, which are non-selective divalent cation channels, permeable for among others  $Zn^{2+}$ ,  $Mg^{2+}$ , and  $Ca^{2+}$  [133, 134]. The protein subfamily TRPM is related to the TRP superfamily, consisting of cation transporters of which most respond to physical or chemical stimuli as reviewed extensively [88, 135–137].

TRPM7 is expressed ubiquitously in the body and considered the main gateway of  $Mg^{2+}$  into metazoan cells. Cells deficient of TRPM7 have decreased intracellular  $Mg^{2+}$  levels and require  $Mg^{2+}$  supplementation when cultured in vitro. [138, 139] The TRPM6 channel is more uniquely expressed with high levels in the intestines and kidney, contributing to  $Mg^{2+}$  homeostasis in vivo [133, 140, 141].

No evidence has been found for prokaryotic TRP orthologues, yet different TRP subfamilies are found in unicellular eukaryotic organisms, such as algae (TRPP and TRPV), amoebozoans (TRPP and TRPML), and choanoflagellates, which are the closest single cell relatives to the metazoa (TRPML, TRPA, TRPV, TRPVL, TRPC, and TRPM), suggesting that the TRP channels evolved during the origin of the eukaryotes [142, 143]. Within the TRPM family, the members TRPM6 and TRPM7 stand out, as they are specialised in  $Mg^{2+}$  transport, yet structurally they are very similar to the other members of the TRPM channels (Fig. 7). They share a conserved N-terminus, the melastatin homology region, that has been postulated to bind ligands and modulate channel activity, through a coiled coil region at the C-terminal domain of the protein [144–147]. Furthermore, the proteins all contain a TRP domain, a sequence of approximately 25 amino acids. This domain has been shown important in TRPV, -C, -M, and -L channels for their activity [148]. It binds to phosphatidylinositol (4,5) bisphosphate (PIP2), a common modulator of channel activity, although in some, it activates the channel, whereas in others causes, inhibition [135, 148]. The selectivity pore of TRPM7 is defined by its motif Phe-Gly-Glu (position 1045–47 in murine TRPM7) (Fig. 7A), facilitating  $Mg^{2+}$  and  $Ca^{2+}$  permeability. Mutagenesis of Glu1047 to Gln, which is found in this motif in TRPM4, a monovalent cation transporter, abolishes the divalent permeability [144].

**Fig. 7** Structure of TRPM7; **A** Structure of the homotetramer transient receptor potential melastatin type 7 (TRPM7, PDB: 5ZX5) in complex with  $Mg^{2+}$  (purple spheres, left panel) with one monomer highlighted. Right panel: zoom in on residues of the selectivity pore Phe-Gly-Glu that bind  $Mg^{2+}$  **B** Schematic depiction of the monomer of TRPM7 using same colours as in A to reflect the approximate structure and location



TRPM6 and TRPM7 are specialised channels in the TRPM family for two major reasons. The channels form homo or heterotetramer structures, which is necessary for their activation. Yet, TRPM6 homotetramers are considered inactive, inferring that TRPM7 expression is always concomitant with TRPM6 [21, 134]. Secondly, both proteins are “chanzymes”, having a channel function and kinase domain. The structure of the kinase domain has not been solved yet, but from electrophysiological studies, the domain seems important for binding of ligands, such as  $MgATP$ , and is crucial for channel activity [149–152]. Deletion of the kinase domain leads to embryonic lethality in mice, while heterozygous deletion allows maturation of the animals, yet leads to defects in the heart teeth and leads to decrease  $Mg^{2+}$  levels in the body [149, 153, 154]. In addition to  $Mg^{2+}$  and  $MgATP$ ,  $Zn^{2+}$  and  $Ca^{2+}$  also directly regulate channel activity.  $Mg^{2+}$  is postulated to bind to the linker between the channel and kinase domain, whereas there is a  $Zn^{2+}$  binding motif located in the kinase domain, consisting of two histidines and cysteines [155]. Oxidation of the cysteines, for example

induced by  $H_2O_2$  exposure, results in dissociation of  $Zn^{2+}$  ions from the channel with inactivation as a consequence. These cysteines may, therefore, act as sensors for oxidative stress. Closing the TRPM7 channel may prevent further cell damage, as increased cytosolic  $Mg^{2+}$  levels are associated with increased ROS levels [156–158]. Furthermore,  $Zn^{2+}$  influx has been implicated with neurotoxicity, while increased intracellular levels may induce  $Ca^{2+}$ -mediated caspase activity and ultimately cell death [159–161].

## Conclusions

$Mg^{2+}$  homeostasis in both prokaryotes and eukaryotes is orchestrated by the interplay of various  $Mg^{2+}$  channels and transporters, indicating a high degree of regulatory pathways. Although the structure of individual  $Mg^{2+}$  transporters have significantly changed, the motifs that form the selective pore in CorA, CorB/C, and MgtE have all been conserved in their eukaryotic counterparts. Incredibly, the overall tertiary and



quaternary structure for CorA and CorB/C have been sustained in MRS2 and CNNM proteins respectively despite low amino acid identity. This demonstrates the importance of these structures for  $Mg^{2+}$  specific transport.

Despite these similarities, it is conspicuous that in unicellular fungi, such as *S. cerevisiae*, CorA orthologues play an important role in  $Mg^{2+}$  homeostasis with many paralogues/homologues present in different subcellular compartments. However, metazoa only have the CorA orthologue, Mrs2, in mitochondria and do not have an evolutionary conserved CorA-like protein at the plasma membrane. Cellular  $Mg^{2+}$  influx is mainly orchestrated via TRPM6 and -7 channels in these organisms, suggesting that these channels may have an evolutionary advantage compared to CorA orthologues. TRPM6 and -7 are responsive to different hormones and ligands [138, 162, 163] which allows fine-tuning of their activity. Moreover, they contain a kinase domain of which the function of  $Mg^{2+}$  homeostasis is still poorly understood, despite extensive research. Unravelling the function of this domain, as well as further identification of interaction partners and regulatory pathways may shine light upon the loss of CorA orthologues in favour of TRPM6 and -7 channels in metazoa.

To gain more insights into the similarities and differences between pro- and eukaryotic  $Mg^{2+}$  channels/transporters, a few approaches could be considered. First of all, the structures of several eukaryotic  $Mg^{2+}$  channels and transporters have not completely resolved, including SLC41 and MgtE proteins. To date, only prediction tools (AlphaFold) have provided structural information of SLC41 proteins, but ultimately cryo-EM or X-ray crystallography is required to elucidate the overall structures. Transport characteristics, e.g. permeation or gating dynamics, could be investigated if structures are available. This would especially be valuable for SLC41 proteins, because they lack the CBS domains compared to MgtE channels. Second, extensive phylogenetic tracing would allow to determine the evolutionary link of SLC41 and MgtE proteins, which is particularly interesting as MgtE orthologues appear to be missing in various phyla, such as land plants and fungi. In addition, it would be important to examine whether MgtA/B orthologues exist in eukaryotes. MgATPases have been postulated to be present in vertebrates, but have not been identified on a genetic level. Lastly, the mode of action of several transporters is often disputed, frequently due the use of different experimental techniques and models. Transport assays using specific isotopes or fluorescent probes in models such as liposomes directly would significantly contribute to the field. These assays are also valuable to determine the difference between paralogues, e.g. the CNNM or SLC41 proteins.

Of note, transporters discussed in this review may not be the only  $Mg^{2+}$  transporting proteins in eukaryotes. For

instance, Magnesium transporter 1 (MagT1) was postulated as a  $Mg^{2+}$  transporter in *X. laevis* oocytes [164]. It is expressed at the plasma membrane and its expression is increased upon low- $Mg^{2+}$  conditions in HEK293T cells [165]. Yet, mutations in the *MagT1* gene have been linked to N-glycosylation and immunodeficiency [166]. As many plasma membrane proteins are glycosylated, it is possible that MagT1 contributes to  $Mg^{2+}$  homeostasis by modulating  $Mg^{2+}$  channels and transporters at the membrane via glycosylation. Members of the solute carrier proteins 25 (SLC25) are mitochondrial specific antiporters of MgATP and  $HPO_4^-$ , that indeed transport (indirectly)  $Mg^{2+}$  [167]. Although members of these transporters can also transport ADP, free  $Mg^{2+}$  transport has not been observed. Lastly, the proteins Non-imprinted in Prader-Willi/Angelman syndrome (NIPA) 1–4 have been postulated to be  $Mg^{2+}$  transporters [19]. Mutations in the genes are linked to Prader-Willi/Angelman syndrome, resulting in hypogonadism, hypotonia, intellectual disability, growth defects, and childhood obesity [168]. Expression of NIPA protein in heterologous systems, such as the *X. laevis* oocytes, indeed show  $Mg^{2+}$  fluxes that can be ablated upon the introduction of patient mutations [169]. Yet, experimental data confirming the involvement of NIPA proteins in  $Mg^{2+}$  transport in mammalian cells is largely lacking. Extensive reviewing of aforementioned proteins should be performed in homologous cell systems to determine  $Mg^{2+}$  transport function.

In conclusion, to study the structural relationship between  $Mg^{2+}$  transporters in different phyla enables the understanding the origin and function of current mammalian magnesiumotropic proteins. This broadens our current knowledge in  $Mg^{2+}$  homeostasis in health and disease.

**Acknowledgements** We thank M.K. van Goor (Department of Physiology, Radboudumc, Nijmegen, the Netherlands) for help with Chimera.

**Author contributions** G.F., R.B., and J.d.B. conceived the idea of the manuscript, G.F., M.H., and L.C., have written the manuscript. All authors corrected the manuscript and approved the final version.

**Funding** This work was supported by the Netherlands Organization for Scientific Research (NWO Veni 016.186.012) and the European Joint Programme on Rare Diseases (EJPRD2019-40).

**Availability of data and materials** Not applicable.

## Declarations

**Conflict of interest** The authors have no relevant financial or non-financial interests to disclose.

**Ethical approval and consent to participate** Not applicable.

**Consent for publication** Not applicable.



**Open Access** This article is licensed under a Creative Commons Attribution 4.0 International License, which permits use, sharing, adaptation, distribution and reproduction in any medium or format, as long as you give appropriate credit to the original author(s) and the source, provide a link to the Creative Commons licence, and indicate if changes were made. The images or other third party material in this article are included in the article's Creative Commons licence, unless indicated otherwise in a credit line to the material. If material is not included in the article's Creative Commons licence and your intended use is not permitted by statutory regulation or exceeds the permitted use, you will need to obtain permission directly from the copyright holder. To view a copy of this licence, visit <http://creativecommons.org/licenses/by/4.0/>.

## References

- de Baaij JH, Hoenderop JG, Bindels RJ (2015) Magnesium in man: implications for health and disease. *Physiol Rev* 95(1):1–46
- Cowan JA (2002) Structural and catalytic chemistry of magnesium-dependent enzymes. *Biomaterials* 15(3):225–235
- Huang SL, Tsai MD (1982) Does the magnesium(II) ion interact with the alpha-phosphate of ATP? An investigation by oxygen-17 nuclear magnetic resonance. *Biochemistry* 21(5):951–959
- Cowan JA (1995) Biological chemistry of magnesium. VCH Publishers, Weinheim
- Flachner B et al (2004) Role of phosphate chain mobility of MgATP in completing the 3-phosphoglycerate kinase catalytic site: binding, kinetic, and crystallographic studies with ATP and MgATP. *Biochemistry* 43(12):3436–3449
- Vicario PP, Bennun A (1990) Separate effects of Mg<sup>2+</sup>, MgATP, and ATP<sub>4</sub>– on the kinetic mechanism for insulin receptor tyrosine kinase. *Arch Biochem Biophys* 278(1):99–105
- Kühlbrandt W (2004) Biology, structure and mechanism of P-type ATPases. *Nat Rev Mol Cell Biol* 5(4):282–295
- Wang Z, Cole PA (2014) Catalytic mechanisms and regulation of protein kinases. *Methods Enzymol* 548:1–21
- Ador L et al (2004) Mutation and evolution of the magnesium-binding site of a class II aminoacyl-tRNA synthetase. *Biochemistry* 43(22):7028–7037
- Batra VK et al (2006) Magnesium-induced assembly of a complete DNA polymerase catalytic complex. *Structure* 14(4):757–766
- Sosunov V et al (2003) Unified two-metal mechanism of RNA synthesis and degradation by RNA polymerase. *Embo j* 22(9):2234–2244
- Schuwirth BS et al (2005) Structures of the bacterial ribosome at 3.5 Å resolution. *Science* 310(5749):827–834
- Zhong S, Bird A, Kopec RE (2021) The metabolism and potential bioactivity of chlorophyll and metallo-chlorophyll derivatives in the gastrointestinal tract. *Mol Nutr Food Res* 65(7):2000761
- Lee J, Ghosh S, Saier MH Jr (2017) Comparative genomic analyses of transport proteins encoded within the red algae *Chondrus crispus*, *Galdieria sulphuraria*, and *Cyanidioschyzon merolae*(11). *J Phycol* 53(3):503–521
- Feord HK et al (2019) A magnesium transport protein related to mammalian SLC41 and bacterial MgtE contributes to circadian timekeeping in a unicellular green alga. *Genes (Basel)* 10(2):158
- Dalmas O et al (2014) A repulsion mechanism explains magnesium permeation and selectivity in CorA. *Proc Natl Acad Sci* 111(8):3002–3007
- Snavely MD et al (1989) Magnesium transport in *Salmonella typhimurium*: 28Mg<sup>2+</sup> transport by the CorA, MgtA, and MgtB systems. *J Bacteriol* 171(9):4761–4766
- Schindl R et al (2007) Mrs2p forms a high conductance Mg<sup>2+</sup>-selective channel in mitochondria. *Biophys J* 93(11):3872–3883
- Quamme GA (2010) Molecular identification of ancient and modern mammalian magnesium transporters. *Am J Physiol Cell Physiol* 298(3):C407–C429
- Takeda H et al (2014) Structural basis for ion selectivity revealed by high-resolution crystal structure of Mg<sup>2+</sup> channel MgtE. *Nat Commun* 5:5374
- Li M, Jiang J, Yue L (2006) Functional characterization of homo- and heteromeric channel kinases TRPM6 and TRPM7. *J Gen Physiol* 127(5):525–537
- Topala CN et al (2007) Molecular determinants of permeation through the cation channel TRPM6. *Cell Calcium* 41(6):513–523
- Monteilh-Zoller MK et al (2003) TRPM7 provides an ion channel mechanism for cellular entry of trace metal ions. *J Gen Physiol* 121(1):49–60
- Guan B, Chen X, Zhang H (2013) Two-electrode voltage clamp. In: Gamper N (ed) *Ion channels: methods and protocols*. Humana Press, Totowa, pp 79–89
- Hook MJV, Thoreson WB (2014) Whole-cell patch-clamp recording. *Current laboratory methods in neuroscience research*. Springer, Berlin, pp 353–367
- Silver S (1969) Active transport of magnesium in *Escherichia coli*. *Proc Natl Acad Sci USA* 62(3):764–771
- Lusk JE, Kennedy EP (1969) Magnesium transport in *Escherichia coli*. *J Biol Chem* 244(6):1653–1655
- Nelson DL, Kennedy EP (1971) Magnesium transport in *Escherichia coli*. Inhibition by cobaltous ion. *J Biol Chem* 246(9):3042–3049
- Hmiel SP et al (1986) Magnesium transport in *Salmonella typhimurium*: characterization of magnesium influx and cloning of a transport gene. *J Bacteriol* 168(3):1444–1450
- Kehres DG, Lawyer CH, Maguire ME (1998) The CorA magnesium transporter gene family. *Microb Comp Genom* 3(3):151–169
- Gibson MM et al (1991) Magnesium transport in *Salmonella typhimurium*: the influence of new mutations conferring Co<sup>2+</sup> resistance on the CorA Mg<sup>2+</sup> transport system. *Mol Microbiol* 5(11):2753–2762
- Hmiel SP et al (1989) Magnesium transport in *Salmonella typhimurium*: genetic characterization and cloning of three magnesium transport loci. *J Bacteriol* 171(9):4742–4751
- Moncrief MB, Maguire ME (1999) Magnesium transport in prokaryotes. *J Biol Inorg Chem* 4(5):523–527
- Eshaghi S et al (2006) Crystal structure of a divalent metal ion transporter CorA at 2.9 Å resolution. *Science* 313(5785):354–357
- Payandeh J, Pai EF (2006) A structural basis for Mg<sup>2+</sup> homeostasis and the CorA translocation cycle. *Embo J* 25(16):3762–3773
- Nordin N et al (2013) Exploring the structure and function of *Thermotoga maritima* CorA reveals the mechanism of gating and ion selectivity in Co<sup>2+</sup>/Mg<sup>2+</sup> transport. *Biochem J* 451(3):365–374
- Cleverley RM et al (2015) The Cryo-EM structure of the CorA channel from *Methanocaldococcus jannaschii* in low magnesium conditions. *Biochim Biophys Acta* 1848(10):2206–2215
- Matthies D et al (2016) Cryo-EM structures of the magnesium channel CorA reveal symmetry break upon gating. *Cell* 164(4):747–756
- Lunin VV et al (2006) Crystal structure of the CorA Mg<sup>2+</sup> transporter. *Nature* 440(7085):833–837
- Payandeh J, Pfoh R, Pai EF (2013) The structure and regulation of magnesium selective ion channels. *Biochim Biophys Acta* 1828(11):2778–2792
- Lerche M et al (2017) Structure and cooperativity of the cytosolic domain of the CorA Mg(2+) channel from *Escherichia coli*. *Structure* 25(8):1175–1186.e4

42. Nemchinova M et al (2021) Asymmetric CorA gating mechanism as observed by molecular dynamics simulations. *J Chem Inf Model* 61(5):2407–2417
43. Kowitz T, Maguire ME (2019) Loss of cytosolic Mg(2+) binding sites in the *Thermotoga maritima* CorA Mg(2+) channel is not sufficient for channel opening. *Biochim Biophys Acta Gen Subj* 1863(1):25–30
44. Knoop V et al (2005) Transport of magnesium and other divalent cations: evolution of the 2-TM-GxN proteins in the MIT superfamily. *Mol Genet Genom* 274(3):205–216
45. Sponder G et al (2010) Lpe10p modulates the activity of the Mrs2p-based yeast mitochondrial Mg2+ channel. *FEBS J* 277(17):3514–3525
46. Gregan J et al (2001) The mitochondrial inner membrane protein Lpe10p, a homologue of Mrs2p, is essential for magnesium homeostasis and group II intron splicing in yeast. *Mol Genet Genom* 264(6):773–781
47. Zsurka G, Gregán J, Schweyen RJ (2001) The human mitochondrial Mrs2 protein functionally substitutes for its yeast homologue, a candidate magnesium transporter. *Genomics* 72(2):158–168
48. Kolisek M et al (2003) Mrs2p is an essential component of the major electrophoretic Mg2+ influx system in mitochondria. *Embo J* 22(6):1235–1244
49. Khan MB et al (2013) Structural and functional characterization of the N-terminal domain of the yeast Mg2+ channel Mrs2. *Acta Crystallogr D* 69(Pt 9):1653–1664
50. Bui DM et al (1999) The bacterial magnesium transporter CorA can functionally substitute for its putative homologue Mrs2p in the yeast inner mitochondrial membrane. *J Biol Chem* 274(29):20438–20443
51. Yamanaka R et al (2016) Mitochondrial Mg2+ homeostasis decides cellular energy metabolism and vulnerability to stress. *Sci Rep* 6(1):30027
52. Merolle L et al (2018) Overexpression of the mitochondrial Mg channel MRS2 increases total cellular Mg concentration and influences sensitivity to apoptosis. *Metallomics* 10(7):917–928
53. EMBL-EBI (2022) TreeFam - database of animal gene trees. <http://www.treefam.org>. Accessed 11th Jan 2022
54. Gebert M et al (2009) A root-expressed magnesium transporter of the MRS2/MGT gene family in *Arabidopsis thaliana* allows for growth in low-Mg2+ environments. *Plant Cell* 21(12):4018–4030
55. Saito T et al (2013) Expression and functional analysis of the CorA-MRS2-ALR-type magnesium transporter family in rice. *Plant Cell Physiol* 54(10):1673–1683
56. Zhao Z et al (2018) Phylogenetic and expression analysis of the magnesium transporter family in pear, and functional verification of PbrMGT7 in pear pollen. *J Hort Sci Biotechnol* 93(1):51–63
57. Tong M et al (2020) Identification and functional analysis of the CorA/MGT/MRS2-type magnesium transporter in banana. *PLoS ONE* 15(10):e0239058
58. Schmitz J et al (2013) Membrane protein interactions between different *Arabidopsis thaliana* MRS2-type magnesium transporters are highly permissive. *Biochim et Biophys Acta (BBA)* 1828(9):2032–2040
59. Lu H-F et al (2020) PhoPQ two-component regulatory system plays a global regulatory role in antibiotic susceptibility, physiology, stress adaptation, and virulence in *Stenotrophomonas maltophilia*. *BMC Microbiol* 20(1):312
60. Kravchenko U et al (2021) The PhoPQ two-component system is the major regulator of cell surface properties, stress responses and plant-derived substrate utilisation during development of peccobacterium versatile-host plant pathosystems. *Front Microbiol*. <https://doi.org/10.3389/fmicb.2020.621391>
61. Johnson CR et al (2001) Generation and characterization of a PhoP homologue mutant of *Neisseria meningitidis*. *Mol Microbiol* 39(5):1345–1355
62. Cromie MJ, Groisman EA (2010) Promoter and riboswitch control of the Mg2+ transporter MgtA from *Salmonella enterica*. *J Bacteriol* 192(2):604–607
63. Cromie MJ et al (2006) An RNA sensor for intracellular Mg(2+). *Cell* 125(1):71–84
64. Håkansson KO (2009) The structure of Mg-ATPase nucleotide-binding domain at 16 Å resolution reveals a unique ATP-binding motif. *Acta Crystallogr D* 65(Pt 11):1181–1186
65. Mirčevová L et al (1979) Activation of Mg-ATPase (Spectrin-Dependent ATPase) by Ca<sup>2+</sup>. *Enzyme* 24:374–382
66. Vrbjar N, Dzurba A, Ziegelhöffer A (1995) Enzyme kinetics and the activation energy of Mg-ATPase in cardiac sarcolemma: ADP as an alternative substrate. *Gen Physiol Biophys* 14(4):313–321
67. Thiyagarajah P, Lim SC (1986) The (Ca<sup>2+</sup> + Mg<sup>2+</sup>)-stimulated ATPase of the rat parotid endoplasmic reticulum. *Biochem J* 235(2):491–498
68. Gandhi CR, Ross DH (1988) Characterization of a high-affinity Mg2+-independent Ca2+-ATPase from rat brain synaptosomal membranes. *J Neurochem* 50(1):248–256
69. Dhalla NS, Zhao D (1989) Possible role of sarcolemmal Ca2+/Mg2+ ATPase in heart function. *Magn Res* 2(3):161–172
70. Szemraj J et al (2005) Magnesium sulfate effect on erythrocyte membranes of asphyxiated newborns. *Clin Biochem* 38(5):457–464
71. Söding J, Biegert A, Lupas AN (2005) The HHpred interactive server for protein homology detection and structure prediction. *Nucleic Acids Res* 33:W244–W248
72. Kolisek M et al (2019) Magnesium extravaganza: a critical compendium of current research into cellular Mg2+ transporters other than TRPM6/7. In: de Tombe P et al (eds) *Reviews of physiology, biochemistry and pharmacology* 176. Springer International Publishing, Cham, pp 65–105
73. Kwasnicka-Crawford DA et al (2005) Characterization of a novel cation transporter ATPase gene (ATP13A4) interrupted by 3q25–q29 inversion in an individual with language delay. *Genomics* 86(2):182–194
74. Vallipuram J, Grenville J, Crawford DA (2010) The E646D-ATP13A4 mutation associated with autism reveals a defect in calcium regulation. *Cell Mol Neurobiol* 30(2):233–246
75. Tan J et al (2011) Regulation of intracellular manganese homeostasis by Kufor-Rakeb syndrome-associated ATP13A2 protein. *J Biol Chem* 286(34):29654–29662
76. van Veen S et al (2020) ATP13A2 deficiency disrupts lysosomal polyamine export. *Nature* 578(7795):419–424
77. Cronin SR, Rao R, Hampton RY (2002) Cod1p/Spf1p is a P-type ATPase involved in ER function and Ca2+ homeostasis. *J Cell Biol* 157(6):1017–1028
78. Will C et al (2010) Targeted deletion of murine Cldn16 identifies extra- and intrarenal compensatory mechanisms of Ca2+ and Mg2+ wasting. *Am J Physiol* 298(5):F1152–F1161
79. Lambie EJ et al (2013) CATP-6, a *C. elegans* Ortholog of ATP13A2 PARK9, Positively Regulates GEM-1, an SLC16A Transporter. *PLoS ONE* 8(10):202
80. Smith RL, Thompson LJ, Maguire ME (1995) Cloning and characterization of MgtE, a putative new class of Mg2+ transporter from *Bacillus firmus* OF4. *J Bacteriol* 177(5):1233–1238
81. Townsend DE et al (1995) Cloning of the mgtE Mg2+ transporter from *Providencia stuartii* and the distribution of mgtE in gram-negative and gram-positive bacteria. *J Bacteriol* 177(18):5350–5354
82. Dann CE 3rd et al (2007) Structure and mechanism of a metal-sensing regulatory RNA. *Cell* 130(5):878–892

83. Hattori M et al (2007) Crystal structure of the MgtE Mg<sup>2+</sup> transporter. *Nature* 448(7157):1072–1075
84. Ignoul S, Eggermont J (2005) CBS domains: structure, function, and pathology in human proteins. *Am J Physiol Cell Physiol* 289(6):C1369–C1378
85. Tomita A et al (2017) ATP-dependent modulation of MgtE in Mg<sup>2+</sup> homeostasis. *Nat Commun* 8(1):148
86. Hattori M et al (2009) Mg<sup>2+</sup>-dependent gating of bacterial MgtE channel underlies Mg<sup>2+</sup> homeostasis. *EMBO J* 28(22):3602–3612
87. Jin F et al (2021) The structure of MgtE in the absence of magnesium provides new insights into channel gating. *PLoS Biol* 19(4):e3001231
88. Sahni J, Song Y, Scharenberg AM (2012) The *B. subtilis* MgtE magnesium transporter can functionally compensate TRPM7-deficiency in vertebrate B-Cells. *PLoS ONE* 7(9):e44452
89. Wabakken T et al (2003) The human solute carrier SLC41A1 belongs to a novel eukaryotic subfamily with homology to prokaryotic MgtE Mg<sup>2+</sup> transporters. *Biochem Biophys Res Commun* 306(3):718–724
90. Sahni J, Nelson B, Scharenberg AM (2007) SLC41A2 encodes a plasma-membrane Mg<sup>2+</sup> transporter. *Biochem J* 401(2):505–513
91. Goytain A, Quamme GA (2005) Functional characterization of human SLC41A1, a Mg<sup>2+</sup> transporter with similarity to prokaryotic MgtE Mg<sup>2+</sup> transporters. *Physiol Genom* 21(3):337–342
92. Kolisek M et al (2008) SLC41A1 is a novel mammalian Mg<sup>2+</sup> carrier. *J Biol Chem* 283(23):16235–16247
93. Kolisek M et al (2012) Human gene SLC41A1 encodes for the Na<sup>+</sup>/Mg<sup>2+</sup> exchanger. *Am J Physiol Cell Physiol* 302(1):C318–C326
94. Mastrototaro L et al (2016) Solute carrier 41A3 encodes for a mitochondrial Mg<sup>2+</sup> efflux system. *Sci Rep* 6:27999
95. Barry G (2013) Hall, building phylogenetic trees from molecular data with MEGA. *Mol Biol Evol* 30(5):1229–1235. <https://doi.org/10.1093/molbev/mst012>
96. Goytain A, Quamme GA (2005) Functional characterization of the mouse [corrected] solute carrier, SLC41A2. *Biochem Biophys Res Commun* 330(3):701–705
97. Sahni J, Scharenberg AM (2013) The SLC41 family of MgtE-like magnesium transporters. *Mol Aspects Med* 34(2–3):620–628
98. Arjona FJ et al (2019) SLC41A1 is essential for magnesium homeostasis in vivo. *Pflugers Arch* 471(6):845–860
99. de Baaij JH et al (2013) Elucidation of the distal convoluted tubule transcriptome identifies new candidate genes involved in renal Mg<sup>2+</sup> handling. *Am J Physiol Renal Physiol* 305(11):F1563–F1573
100. Hess MW et al (2016) Inulin significantly improves serum magnesium levels in proton pump inhibitor-induced hypomagnesaemia. *Aliment Pharmacol Ther* 43(11):1178–1185
101. Chen YS et al (2021) Crystal structure of an archaeal CorB magnesium transporter. *Nat Commun* 12(1):4028
102. Huang Y et al (2021) Structural basis for the Mg<sup>2+</sup> recognition and regulation of the CorC Mg<sup>2+</sup> transporter. *Sci Adv* 7(7):eabe6140
103. Wang C-Y et al (2003) Molecular cloning and characterization of a novel gene family of four ancient conserved domain proteins (ACDP). *Gene* 306:37–44
104. Wang CY et al (2004) Molecular cloning and characterization of the mouse Acdp gene family. *BMC Genomics* 5(1):7
105. Goytain A, Quamme GA (2005) Functional characterization of ACDP2 (ancient conserved domain protein), a divalent metal transporter. *Physiol Genom* 22(3):382–389
106. Hirata Y et al (2014) Mg<sup>2+</sup>-dependent interactions of ATP with the cystathionine-β-Synthase (CBS) domains of a magnesium transporter \*. *J Biol Chem* 289(21):14731–14739
107. Stuver M et al (2011) CNNM2, encoding a basolateral protein required for renal Mg<sup>2+</sup> handling, is mutated in dominant hypomagnesemia. *Am J Hum Genet* 88(3):333–343
108. Sponder G et al (2016) Human CNNM2 is not a Mg<sup>2+</sup> transporter per se. *Pflügers Arch Eur J Physiol* 468(7):1223–1240
109. de Baaij JH et al (2012) Membrane topology and intracellular processing of cyclin M2 (CNNM2). *J Biol Chem* 287(17):13644–13655
110. Arjona FJ, de Baaij JHF (2018) CrossTalk opposing view: CNNM proteins are not Na<sup>+</sup>/Mg<sup>2+</sup> exchangers but Mg<sup>2+</sup> transport regulators playing a central role in transepithelial Mg<sup>2+</sup> (re) absorption. *J Physiol* 596(5):747–750
111. Funato Y et al (2018) CrossTalk proposal: CNNM proteins are Na<sup>+</sup>/Mg<sup>2+</sup> exchangers playing a central role in transepithelial Mg<sup>2+</sup> (re)absorption. *J Physiol* 596(5):743–746
112. Hardy S et al (2015) The protein tyrosine phosphatase PRL-2 interacts with the magnesium transporter CNNM3 to promote oncogenesis. *Oncogene* 34(8):986–995
113. Zhang H et al (2017) PRL3 phosphatase active site is required for binding the putative magnesium transporter CNNM3. *Sci Rep* 7(1):48
114. Giménez-Mascarell P et al (2017) Structural basis of the oncogenic interaction of phosphatase PRL-1 with the magnesium transporter CNNM2. *J Biol Chem* 292(3):786–801
115. Hardy S et al (2019) Magnesium-sensitive upstream ORF controls PRL phosphatase expression to mediate energy metabolism. *Proc Natl Acad Sci USA* 116(8):2925–2934
116. Zolotarov Y et al (2021) ARL15 modulates magnesium homeostasis through N-glycosylation of CNNMs. *Cell Mol Life Sci* 78(13):5427–5445
117. Kollwe A et al (2021) The molecular appearance of native TRPM7 channel complexes identified by high-resolution proteomics. *Elife* 10:e68544
118. Arjona FJ et al (2014) CNNM2 mutations cause impaired brain development and seizures in patients with hypomagnesemia. *PLoS Genet* 10(4):e1004267
119. Franken GAC et al (2021) The phenotypic and genetic spectrum of patients with heterozygous mutations in cyclin M2 (CNNM2). *Hum Mutat* 42(4):473–486
120. Funato Y, Yamazaki D, Miki H (2017) Renal function of cyclin M2 Mg<sup>2+</sup> transporter maintains blood pressure. *J Hypertens* 35(3):585–592
121. Franken GAC et al (2021) Cyclin M2 (CNNM2) knockout mice show mild hypomagnesaemia and developmental defects. *Sci Rep* 11(1):8217
122. Accogli A et al (2019) CNNM2 homozygous mutations cause severe refractory hypomagnesemia, epileptic encephalopathy and brain malformations. *Eur J Med Genet* 62(3):198–203
123. Yamazaki D et al (2013) Basolateral Mg<sup>2+</sup> extrusion via CNNM4 mediates transcellular Mg<sup>2+</sup> transport across epithelia: a mouse model. *PLoS Genet* 9(12):e1003983
124. Funato Y et al (2014) Membrane protein CNNM4-dependent Mg<sup>2+</sup> efflux suppresses tumor progression. *J Clin Invest* 124(12):5398–5410
125. Parry DA et al (2009) Mutations in CNNM4 Cause Jalili Syndrome, consisting of autosomal-recessive cone-rod dystrophy and amelogenesis imperfecta. *Am J Human Genet* 84(2):266–273
126. Prasov L et al (2020) Expanding the genotypic spectrum of Jalili syndrome: Novel CNNM4 variants and uniparental isodisomy in a north American patient cohort. *Am J Med Genet A* 182(3):493–497
127. Corral-Rodríguez M et al (2014) Nucleotide binding triggers a conformational change of the CBS module of the magnesium transporter CNNM2 from a twisted towards a flat structure. *Biochem J* 464(1):23–34



128. Giménez-Mascarell P et al (2019) Structural insights into the intracellular region of the human magnesium transport mediator CNNM4. *Int J Mol Sci* 20(24):6279
129. Chen YS et al (2020) Mg(2+)-ATP Sensing in CNNM, a putative magnesium transporter. *Structure* 28(3):324–335.e4
130. Chen YS et al (2018) The cyclic nucleotide-binding homology domain of the integral membrane protein CNNM mediates dimerization and is required for Mg(2+) efflux activity. *J Biol Chem* 293(52):19998–20007
131. Giménez-Mascarell P et al (2019) Current structural knowledge on the CNNM family of magnesium transport mediators. *Int J Mol Sci* 20(5):1135
132. Maruyama T et al (2018) Functional roles of Mg<sup>2+</sup> binding sites in ion-dependent gating of a Mg<sup>2+</sup> channel, MgtE, revealed by solution NMR. *Elife* 7:e31596
133. Luongo F et al (2018) TRPM6 is essential for magnesium uptake and epithelial cell function in the colon. *Nutrients* 10(6):784
134. Schmitz C et al (2005) The channel kinases TRPM6 and TRPM7 are functionally nonredundant. *J Biol Chem* 280(45):37763–37771
135. Ramsey IS, Delling M, Clapham DE (2006) An introduction to TRP channels. *Annu Rev Physiol* 68:619–647
136. Zheng J (2013) Molecular mechanism of TRP channels. *Compr Physiol* 3(1):221–242
137. Falcón D et al (2019) TRP channels: current perspectives in the adverse cardiac remodeling. *Front Physiol*. <https://doi.org/10.3389/fphys.2019.00159>
138. Zou ZG et al (2019) TRPM7, magnesium, and signaling. *Int J Mol Sci* 20(8):1877
139. Chubanov V et al (2016) Epithelial magnesium transport by TRPM6 is essential for prenatal development and adult survival. *Elife* 5:e20914
140. Woudenberg-Vrenken TE et al (2011) Transient receptor potential melastatin 6 knockout mice are lethal whereas heterozygous deletion results in mild hypomagnesemia. *Nephron Physiol* 117(2):11–19
141. Walder RY et al (2009) Mice defective in *Trpm6* show embryonic mortality and neural tube defects. *Hum Mol Genet* 18(22):4367–4375
142. Himmel NJ, Cox DN (1933) Transient receptor potential channels: current perspectives on evolution, structure, function and nomenclature. *Proc R Soc B* 2020(287):20201309
143. Peng G, Shi X, Kadowaki T (2015) Evolution of TRP channels inferred by their classification in diverse animal species. *Mol Phylogenet Evol* 84:145–157
144. Duan J et al (2018) Structure of the mammalian TRPM7, a magnesium channel required during embryonic development. *Proc Natl Acad Sci* 115(35):E8201–E8210
145. Huang Y et al (2019) Ligand recognition and gating mechanism through three ligand-binding sites of human TRPM2 channel. *Elife* 8:e50175
146. Winkler PA et al (2017) Electron cryo-microscopy structure of a human TRPM4 channel. *Nature* 552(7684):200–204
147. Huang Y et al (2018) Architecture of the TRPM2 channel and its activation mechanism by ADP-ribose and calcium. *Nature* 562(7725):145–149
148. Rohacs T (2014) Phosphoinositide regulation of TRP channels. *Handb Exp Pharmacol* 223:1143–1176
149. Ryazanova LV et al (2010) TRPM7 is essential for Mg(2+) homeostasis in mammals. *Nat Commun* 1:109
150. Demeuse P, Penner R, Fleig A (2006) TRPM7 channel is regulated by magnesium nucleotides via its kinase domain. *J Gen Physiol* 127(4):421–434
151. Chokshi R, Matsushita M, Kozak JA (2012) Detailed examination of Mg<sup>2+</sup> and pH sensitivity of human TRPM7 channels. *Am J Physiol Cell Physiol* 302(7):C1004–C1011
152. Nadler MJ et al (2001) LTRPC7 is a Mg-ATP-regulated divalent cation channel required for cell viability. *Nature* 411(6837):590–595
153. Ogata K et al (2017) The crucial role of the TRPM7 kinase domain in the early stage of amelogenesis. *Sci Rep* 7(1):18099
154. Rios FJ et al (2020) Chanzyme TRPM7 protects against cardiovascular inflammation and fibrosis. *Cardiovasc Res* 116(3):721–735
155. Inoue H et al (2021) The zinc-binding motif of TRPM7 acts as an oxidative stress sensor to regulate its channel activity. *J Gen Physiol* 153(6):e202012708
156. Chen H-C et al (2012) A key role for Mg<sup>2+</sup> in TRPM7's control of ROS levels during cell stress. *Biochem J* 445(3):441–448
157. Hashizume O et al (2020) Excessive Mg(2+) impairs intestinal homeostasis by enhanced production of adenosine triphosphate and reactive oxygen species. *Antioxid Redox Signal* 33(1):20–34
158. Tamura M, Kanno M, Kai T (2001) Destabilization of neutrophil NADPH oxidase by ATP and other trinucleotides and its prevention by Mg<sup>2+</sup>. *Biochim et Biophys Acta (BBA)* 1510(1–2):270–277
159. Inoue K, Branigan D, Xiong Z-G (2010) Zinc-induced neurotoxicity mediated by transient receptor potential melastatin 7 channels. *J Biol Chem* 285(10):7430–7439
160. Aarts M et al (2003) A key role for TRPM7 channels in anoxic neuronal death. *Cell* 115(7):863–877
161. Marchi S et al (2018) Mitochondrial and endoplasmic reticulum calcium homeostasis and cell death. *Cell Calcium* 69:62–72
162. Thebault S et al (2009) EGF increases TRPM6 activity and surface expression. *J Am Soc Nephrol* 20(1):78–85
163. Nair AV et al (2012) Loss of insulin-induced activation of TRPM6 magnesium channels results in impaired glucose tolerance during pregnancy. *Proc Natl Acad Sci USA* 109(28):11324–11329
164. Goytain A, Quamme GA (2005) Identification and characterization of a novel mammalian Mg<sup>2+</sup> transporter with channel-like properties. *BMC Genom* 6:48
165. Zhou H, Clapham DE (2009) Mammalian *MagT1* and *TUSC3* are required for cellular magnesium uptake and vertebrate embryonic development. *Proc Natl Acad Sci* 106(37):15750–15755
166. Blommaert E et al (2019) Mutations in *MAGT1* lead to a glycosylation disorder with a variable phenotype. *Proc Natl Acad Sci* 116(20):9865–9870
167. Kunji ERS et al (2020) The SLC25 carrier family: important transport proteins in mitochondrial physiology and pathology. *Physiology* 35(5):302–327
168. Cassidy SB et al (2012) Prader-Willi syndrome. *Genet Med* 14(1):10–26
169. Goytain A et al (2007) NIPA1(SPG6), the basis for autosomal dominant form of hereditary spastic paraplegia, encodes a functional Mg<sup>2+</sup> transporter. *J Biol Chem* 282(11):8060–8068

**Publisher's Note** Springer Nature remains neutral with regard to jurisdictional claims in published maps and institutional affiliations.